



Magma transport and storage at Piton de La Fournaise (La Réunion) between 1972 and 2007: A review of geophysical and geochemical data

Aline Peltier^{a,b,*}, Patrick Bachèlery^a, Thomas Staudacher^b

^a Laboratoire GéoSciences Réunion, Université de La Réunion, Institut de Physique du Globe de Paris, CNRS, UMR 7154-Géologie des Systèmes Volcaniques, 15 avenue René Cassin, BP 97715 Saint-Denis cedex 9, La Réunion, France

^b Observatoire Volcanologique du Piton de la Fournaise, Institut de Physique du Globe de Paris, CNRS, UMR 7154-Géologie des Systèmes Volcaniques, 14 RN3, le 27^{ème} km, 97418, La Plaine des Cafres, La Réunion, France

ARTICLE INFO

Article history:

Received 23 June 2008

Accepted 4 December 2008

Available online 1 January 2009

Keywords:

Piton de La Fournaise
eruptive cycle
volcano monitoring
ground deformation
GPS
geochemistry
magma storage
magma transfer

ABSTRACT

Since the middle of the 20th century, improvement in volcano monitoring techniques has provided large data sets that can be used to evaluate the evolution of magma plumbing systems. At Piton de La Fournaise volcano, abundant eruptive activity and a dense monitoring network are especially conducive to such research. Analysis of the extensive set of geophysical and geochemical data associated with the last 35 years of activity provides new insights into magma transport and storage at Piton de La Fournaise. Two periods of frequent eruptions separated by 6 years of inactivity can be distinguished: 1972–1992 and 1998–2007. Considering these two periods, we show evidence of major changes in the shallow plumbing system in 2000. During 1972–1992 and 1998–2000, lava compositions and weak long term eruptive precursors (lasting few days to three weeks), characterized by no significant summit inflation and about ten volcano-tectonic earthquakes per day, suggest that eruptions were fed by the progressive drainage of an occasionally recharged shallow magma reservoir. Geophysical evidence of shallow magma reservoir recharge was only recorded in 1986 and 1998. In contrast, from 2000 to 2007, geophysical data highlight the appearance of long-term precursors (1 to 5 months of summit inflation and strong seismicity, up to one hundred events per day) preceding cycles of successive eruptions. Each cycle of eruptions was characterized by a sequence (3 to 10 months in duration) of summit and near-summit, proximal, eruptions, and ended with a distal, low-altitude oceanite (olivine abundances >20 vol.%) eruption on the eastern flank of the volcano. Within each of these eruptive cycles, lavas became progressively more magnesian over time. The preferential motion of the eastern flank caused by continuous recharging of the shallow reservoir since 2000 would favour the occurrence of distal eruptions towards this flank at the end of a cycle.

© 2008 Elsevier B.V. All rights reserved.

1. Introduction

The frequent eruptive activity and dense monitoring network at Piton de La Fournaise volcano (La Réunion, Indian Ocean) allow for detailed study of the evolution of the volcano's magma transport and storage system over time. Systematic observations of the volcano since 1930 indicate an average of one eruption per year. Since 1998, the frequency of eruptions seems to increase with a mean of two eruptions per year. This apparent increase of eruptive frequency could only reflect a less detailed observation of volcanic activity before the 1970's. During the 20th century, long period of repose (>2 years)

occurred in 1921–1924, 1939–1942, 1966–1972 and 1992–1998. The two longest repose periods (six years) allowed us to define two major active periods for the last 35 years: 1972–1992 and 1998–2007. Since the Volcanological Observatory of Piton de La Fournaise (OVPF) was established in 1980, visual observations were supplemented by geophysical and geochemical measurements. Between 1972 and 2007, 51 of 65 eruptions that occurred were well-documented with seismic and ground deformation data recorded by the OVPF. Eruptive activity at Piton de la Fournaise has been the subject of many studies in many domains, like geochemistry, deformation, seismology and structural analysis. Most of these studies have focused on short time periods that include only one or a few eruptions, and the dynamics of magma transfer and storage over time at Piton de La Fournaise have remained ambiguous. Several hypotheses have been proposed concerning the shallow magma storage. *Lénat and Bachèlery (1990)* suggested the presence of an array of sills and dykes slowly cooling at 0.5–1.5 km beneath the Dolomieu crater whereas *Nercessian et al. (1996)* and *Peltier et al. (2007, 2008)* evidenced by seismic

* Corresponding author. Present address: Institut de Physique du Globe de Paris, CNRS, UMR 7154-Géologie des Systèmes Volcaniques, 4 place jussieu, 75005 Paris, France. Tel.: +33 1 44 27 25 06; fax: +33 1 44 27 73 85.

E-mail addresses: peltier@ipgp.jussieu.fr (A. Peltier), Patrick.Bachelery@univ-reunion.fr (P. Bachèlery), Thomas.Staudacher@univ-reunion.fr (T. Staudacher).

tomography and deformation data the presence of a single shallow reservoir at about 2.5 km depth. So, fundamental questions concerning the presence or absence of a well developed shallow magma system, its geometry, its location, and the connections with deeper magma reservoirs are still debated. The aim of this research is to evaluate eruptive activity at Piton de La Fournaise during the well documented eruptive periods of 1972–1992 and 1998–2007 through an interdisciplinary analysis of deformation, petrological and geochemical data, in order to study the evolution of magma transfer and storage during this time period.

2. Piton de La Fournaise context

2.1. Geological settings

Piton de La Fournaise is located on La Réunion Island, in the SW part of the Indian Ocean (Fig. 1a). It was built on the flanks of two older inactive volcanoes: Piton des Neiges and Les Alizés (Lénat et al., 2001),

located on the western and the eastern parts of the island, respectively (Fig. 1b). The evolution of Piton de La Fournaise was marked by the formation of successive concentric calderas (Bachèlery, 1981; Bachèlery and Mairine, 1990). With few exceptions, recent activity has been located inside the Enclos Fouqué caldera, which formed about 4500 years ago (Fig. 1c; Bachèlery, 1981). Eruptions within Enclos Fouqué have contributed to the formation of a 400 m high summit cone, 3 km wide at its base, in the central part of the caldera. Two craters cut the summit of this cone: the Dolomieu crater in the east and the Bory crater in the west (Fig. 1c). The spatial distribution of historical eruptive fissures defines two curved rift zones directed to the NE and SE (oriented N10 and N170, respectively) that are connected to the central cone (Fig. 1c; Bachèlery, 1981). Since 1998, the eruptive system has been characterized by two preferential feeding pathways striking N25–30 and N120 (Fig. 1c; Michon et al., 2007a). Eruptions on Piton de La Fournaise are focused in three areas. Since 1972, 68% of eruptions began with the opening of en-echelon fissures close to the top of the central cone and migrated down slope on the central cone flanks (proximal

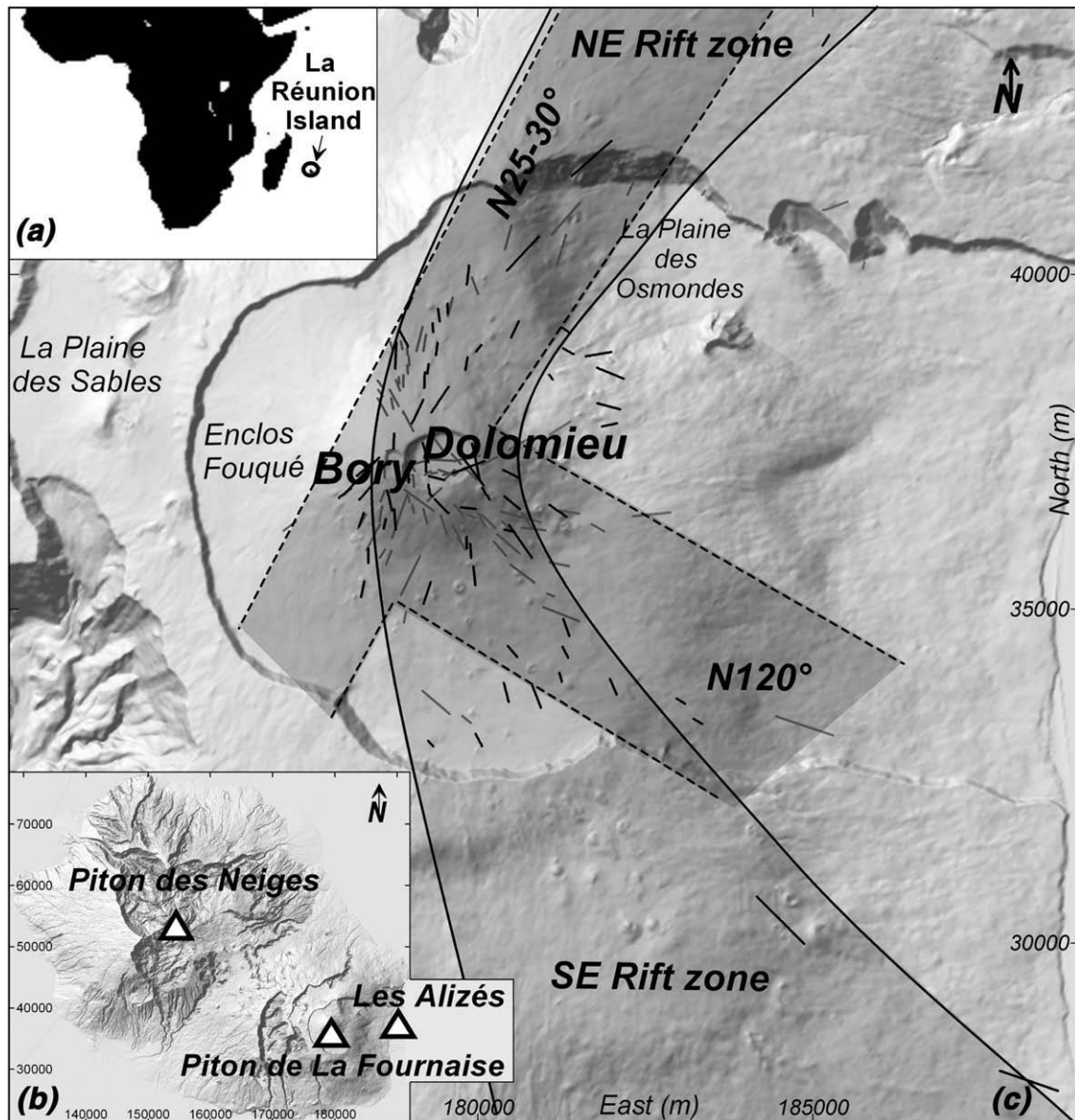


Fig. 1. (a) Location of La Réunion Island. (b) Map of La Réunion Island showing the location of volcanoes. (c) Location of the 1972–1992 (black) and 1998–2007 (grey) eruptive fissures on Piton de La Fournaise (Gauss Laborde Réunion coordinates, meters). Black and dotted lines delimit rift zones, after Bachèlery (1981) and Michon et al. (2007a), respectively.

eruptions). Activity generally stabilized on the lowest of the eruptive fissures, usually at the base of the summit cone. In some cases an eruptive fissure opened first in either Bory or Dolomieu crater, but activity there ceased quickly when flank fissures ensued. Another 21% of eruptions occurred in Dolomieu crater (summit eruptions). Finally, 11% of eruptions occurred more than 4 km from the summit, outside of the summit cone (distal eruptions).

2.2. Nature of emitted lavas

Piton de La Fournaise lavas have major element compositions that are transitional between alkalic and tholeiitic basalts (Coombs, 1963; Upton and Wadsworth, 1965; Upton and Wadsworth, 1966; Upton and Wadsworth, 1972; Ludden, 1978) and have a common homogeneous mantle source (Fisk et al., 1988; Graham et al., 1990; Staudacher et al., 1990; Albarède et al., 1997; Vlastélic et al., 2005; Bosch et al., 2008). Compositions are modified during magma transport and storage by differentiation (Boivin and Bachèlery, 2004; Famin et al., 2008), contamination with host rocks (Vlastélic et al., 2005) or incorporation of olivine crystals (Albarède and Tamagnan, 1988).

Based on bulk major element compositions, four types of lavas have been distinguished at Piton de La Fournaise since the beginning of its activity at 0.5 Ma (Upton and Wadsworth, 1972; Ludden, 1978; Albarède and Tamagnan, 1988; Albarède et al., 1997). The first, and the most abundant group (~65%), is called “Steady State Basalts” (SSB); SSB are transitional basalts which are chemically homogeneous and exhibit little compositional variability (5–8 wt.% MgO; 0.5–1 wt.% K₂O; 10–12 wt.% CaO). The second group includes the olivine-rich basalts (Fo_{85–83}) which are commonly interpreted as derived from SSB by olivine accumulation (8–28 wt.% MgO; 0.4–0.7 wt.% K₂O; 5–11 wt.%

CaO). Following Boivin and Bachèlery (2009–this issue), we adopted the term “oceanite”, first introduced by Lacroix (1912), to designate melanocratic basalts containing a large amount of accumulated olivine megacrysts (>20%). The presence of kink-bands in olivine crystals, mineral-melt Fe/Mg disequilibria and anomalous incompatible element ratios were interpreted as evidences of a xenocryst origin for most of the olivine crystals contained in these lavas (Albarède and Tamagnan, 1988). By contrast, Famin et al. (2008) propose that xenocryst incorporation of host rocks is not necessary to explain the composition of the February and December 2005 oceanite lavas. Combining the study of melt inclusions, fluid inclusions and bulk rock chemical compositions these authors suggest that the olivine crystals contained in these oceanite lavas crystallised at shallow depth (<2600 m depth). The third compositional class is an “evolved” group mainly represented in early Piton de La Fournaise lavas, resulting from shallow crystal fractionation from a SSB-type magma (1–5 wt.% MgO; 1–4 wt.% K₂O; 1.8–10 wt.% CaO). Finally, the fourth group is an “Abnormal Group” (AbG) enriched in Mg, Fe, Ti, Na and K and depleted in Ca and Si compared with SSB (7.5–10 wt.% MgO; 0.9–1.2 wt.% K₂O; 8.5–10 wt.% CaO). AbG lavas have erupted during prehistoric distal eruptions and during only one proximal historic eruption (1998 Hudson eruption). Most of the historic lavas belong to the SSB and the “oceanite” groups, some of which show a slight differentiation according to the trend defined by the “evolved” group.

2.3. Monitoring network

Since 1980, monitoring at Piton de La Fournaise has been conducted by the “Institut de Physique du Globe de Paris” with the establishment of the Volcanological Observatory of Piton de La

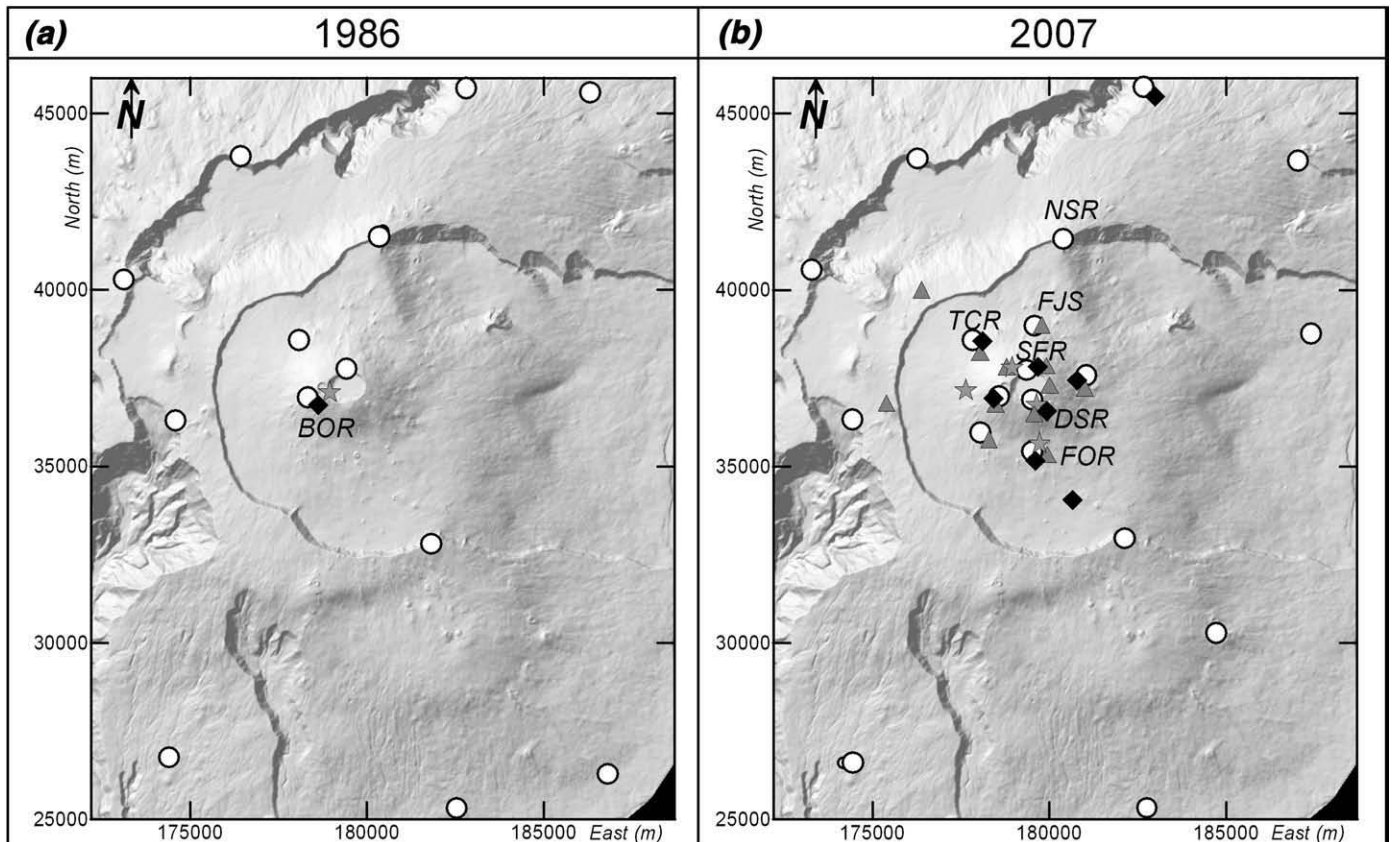


Fig. 2. Permanent monitoring network on Piton de La Fournaise (a) in 1986 (after Delorme et al., 1989) and (b) in 2007. Locations are shown for extensometer stations (grey asterisks), tiltmeter stations (black diamonds) GPS stations (grey triangles) and seismic stations (white circles). Stations discussed in the text are labelled. In the text, the name is followed by *i* for tiltmeter stations, *x* for extensometer stations and *g* for GPS stations. Note that additional seismic stations are located stations.

Table 1
Summary of the 1972–2007 eruptions.

Number	Type	Beginning of eruption	End of eruption	Location	Elevation (m)	Emitted volume ($\times 10^6 \text{ m}^3$)	Lava type
1	E	9(?)–Jun-72	11(?)–Jun-72	S flank	2540–2200	0.27	Poorly phyrlic
2	E	25(?)–Jul-72	17(?)–Aug-72	E NE flank	2200–1760	2.9	Poorly phyrlic
3	E	7(?)–Sep-72	26(?)–Sep-72	N flank	2150–2100	4	Poorly phyrlic
4	E	10(?)–Oct-72	27(?)–Oct-72	S SE flank	1800	1.1	Poorly phyrlic
		27(?)–Oct-72	2(?)–Nov-72	S SE flank	1740	0.16	Poorly phyrlic
		1(?)–Nov-72	14(?)–Nov-72	S SE flank	1680	0.5	Poorly phyrlic
		2(?)–Nov-72	6(?)–Nov-72	S SE flank	1740–1720	0.02	Oceanite
		7(?)–Nov-72	9(?)–Nov-72	S SE flank	1750	0.02	Oceanite
		9(?)–Nov-72	16(?)–Nov-72	S SE flank	1755	2.5	Oceanite
		15(?)–Nov-72	10(?)–Dec-72	S SE flank	1765	5	Oceanite
5	E	10-May-73	28-May-73	Dolomieu (W)	2380	1.6	Poorly phyrlic
6	E	4-Nov-75	18-Nov-75	Dolomieu	2380	1.4	Poorly phyrlic
7	E	18-Dec-75	18-Dec-75	Dolomieu + E SE flank	2350–2220	0.03	Poorly phyrlic
		19-Dec-75	25-Jan-76	E SE flank	2115–2020	1.3	Poorly phyrlic
8	E	12-Jan-76	25-Jan-76	S SE flank	1490	0.8	Poorly phyrlic
		18-Jan-76	30-Jan-76	S SE flank	1320	3	Poorly phyrlic
		29-Jan-76	23-Mar-76	S SE flank	1780	6	Poorly phyrlic
		22-Mar-76	31-Mar-76	S SE flank	1840	0.4	Poorly phyrlic
		31-Mar-76	6-Apr-76	S SE flank	1870	0.1	Poorly phyrlic
9	E	2-Nov-76	3-Nov-76	N flank	2250	0.46	Poorly phyrlic
10	E	24-Mar-77	24-Mar-77	S SE flank	2500–2000	0.06	Poorly phyrlic
11	E	5-Apr-77	16-Apr-77	Dolomieu + NE flank (+ outside of the caldeira)	1900–500	20	Oceanite
12	E	24-Oct-77	17-Nov-77	E flank	2180–1920	23	Olivine-rich
13	E	28-May-79	29-May-79	S SE flank	2100	0.2	Poorly phyrlic
14	E	13-Jul-79	14-Jul-79	N & S flank	??	0.3	Poorly phyrlic
15	E	3-Feb-81	25-Feb-81	Bory + N flank	2540	3	Poorly phyrlic
16	E	26-Feb-81	26-Mar-81	SW flank	2400	4	Poorly phyrlic
17	E	1-Apr-81	5-May-81	NE flank	1900	5	Poorly phyrlic
18	E	4-Dec-83	18-Jan-84	SW flank	2220–2050	8	Poorly phyrlic
		18-Jan-84	18-Feb-84	SW flank	2280	9	Poorly phyrlic
19	E	14-Jun-85	15-Jun-85	W flank	2520	1	Poorly phyrlic
	I	9-Jul-85	9-Jul-85	E flank			
20	E	5-Aug-85	1-Sep-85	N flank	2100	7	Poorly phyrlic
21	E	6-Sep-85	10-Oct-85	Dolomieu + NE flank	2500–2250	14	Poorly phyrlic
22	E	1-Dec-85	3-Dec-85	S flank	2520–2400	0.7	Poorly phyrlic
23	E	29-Dec-85	7-Feb-86	Dolomieu (SW)	2550	7	Poorly phyrlic
24	E	19-Mar-86	5-Apr-86	S SE flank (+ outside of the caldeira)	2500–30	14	Poorly phyrlic
25	E	13-Jul-86	13-Jul-86	Dolomieu (E)	2500	0.27	Poorly phyrlic
26	E	12-Nov-86	13-Nov-86	Dolomieu (E)	2500	0.27	Poorly phyrlic
27	E	26-Nov-86	27-Nov-86	Dolomieu (E)	2500	0.24	Poorly phyrlic
28	E	6-Dec-86	6-Jan-87	Dolomieu (W & E)	2500	2	Poorly phyrlic
	I	6-Jan-87	10-Feb-87	NE flank	1900–1780	10	Poorly phyrlic
	I	2-Jun-87	2-Jun-87	?			
29	E	10-Jun-87	29-Jun-87	Dolomieu (E)	2500–2420	1.5	Poorly phyrlic
30	E	19-Jul-87	20-Jul-87	N & S flank	2050	0.8	Poorly phyrlic
31	E	6-Nov-87	8-Nov-87	N flank	2280–2150	1.6	Poorly phyrlic
32	E	30-Nov-87	1-Jan-88	S flank	2240–1900	10	Poorly phyrlic
33	E	7-Feb-88	2-Apr-88	S flank	2050	8	Poorly phyrlic
	I	20-Apr-88	20-Apr-88	Dolomieu (NE)			
34	E	18-May-88	1-Aug-88	N flank	2300–2200	15	Poorly phyrlic
35	E	31-Aug-88	12-Sep-88	S SW flank	2250	7	Poorly phyrlic
	I	12-Nov-88	12-Nov-88	?			
36	E	14-Dec-88	29-Dec-88	N flank	2250–2100	8	Poorly phyrlic
37	E	18-Jan-90	19-Jan-90	Dolomieu (SE) + SE flank	2510–2450	0.5	Poorly phyrlic
38	E	18-Apr-90	8-May-90	S SE flank	1800	8	Poorly phyrlic
39	E	19-Jul-91	20-Jul-91	Dolomieu (E)	2510	2.8	Poorly phyrlic
	I	7-Dec-91	7-Dec-91	?			
40	E	27-Aug-92	23-Sep-92	Dolomieu (W) + S flank	2530–2050	5.5	Poorly phyrlic
	I	26-Nov-96	26-Nov-96	N flank			
41	E	9-Mar-98	21-Sep-98	N flank	2450–2050	60	Poorly phyrlic
		11-Mar-98	1-Apr-98	W flank	2200	<1	Poorly phyrlic
		8-Aug-98	15-Sep-98	N flank (outside of the caldeira)	1700	<1	Poorly phyrlic
42	E	19-Jul-99	31-Jul-99	Dolomieu + E flank	2500–2100	1.8	Poorly phyrlic
43	E	28-Sep-99	23-Oct-99	Dolomieu + S flank	2500–1850	1.5	Poorly phyrlic
44	E	13-Feb-00	3-Mar-00	N flank	2450–2250	4.1	Poorly phyrlic
45	E	23-Jun-00	30-Jul-00	E SE flank	2100–1820	6	Poorly phyrlic
46	E	12-Oct-00	13-Nov-00	SE flank	2260–2000	9	Poorly phyrlic
47	E	27-Mar-01	4-Apr-01	S SE flank	2450–1940	4.8	Poorly phyrlic
48	E	11-Jun-01	7-Jul-01	SE flank	2450–1800	9.5	Olivine-rich
49	E	5-Jan-02	16-Jan-02	N-E flank+Plaine des Osmondes	1910–1070	13	Oceanite
50	E	16-Nov-02	3-Dec-02	E flank	1850–1500	8	Olivine-rich
51	E	30-May-03	30-May-03	Dolomieu (WSW)	2490	0.14	Poorly phyrlic
		4-Jun-03	9-Jun-03	Dolomieu (WSW)	2490	0.37	Poorly phyrlic
		12-Jun-03	15-Jun-03	Dolomieu (WSW)	2490	0.41	Poorly phyrlic
		22-Jun-03	7-Jul-03	Dolomieu (WSW)	2490	0.36	Poorly phyrlic

Table 1 (continued)

Number	Type	Beginning of eruption	End of eruption	Location	Elevation (m)	Emitted volume ($\times 10^6$ m ³)	Lava type
52	E	22-Aug-03	27-Aug-03	Bory + N flank	2590–2140	6.2	Olivine-rich
53	E	30-Sep-03	1-Oct-03	S flank	2330–2195	1	Poorly phyrlic
	I	6-Nov-03	6-Nov-03	SE flank			
54	E	7-Dec-03	25-Dec-03	Dolomieu (ESE)	2475	1.2	Poorly phyrlic
55	E	8-Jan-04	10-Jan-04	Plaine des Osmondes	1500	1.9	Olivine-rich
56	E	2-May-04	18-May-04	S flank	2525–2000	16	Poorly phyrlic
57	E	12-Aug-04	16-Oct-04	Dolomieu + E flank	2540–1900	20	Poorly phyrlic
58	E	17-Feb-05	26-Feb-05	Plaine des Osmondes	1650–500	18–20	Oceanite
59	E	4-Oct-05	17-Oct-05	Dolomieu (WSW)	2490	1.5	Poorly phyrlic
60	E	29-Nov-05	29-Nov-05	Dolomieu + N flank	2490–2350	1	Poorly phyrlic
61	E	26-Dec-05	18-Jan-06	N flank + Plaine des Osmondes	2025–1600	15–20	Oceanite
62	E	20-Jul-06	14-Aug-06	S flank	2300–2150	2.5–3	Poorly phyrlic
63	E	30-Aug-06	1-Jan-07	Dolomieu (ESE) + E flank	2500	20	Poorly phyrlic
64	E	18-Feb-07	19-Feb-07	Dolomieu	2500	<1	Poorly phyrlic
65	E	30-Mar-07	31-Mar-07	S SE flank	1950–1810	<1	Poorly phyrlic
		2-Apr-07	1-May-07	S SE flank	600–550	140	Oceanite

Type E and I correspond to Eruption and Intrusion, respectively. When no type is mentioned, the eruptive phase is a continuation of the previous activity. For the 1972 eruptions, because of the lack of field observation, the dates are uncertain.

Fournaise and the development of seismic and deformation networks. The first permanent deformation monitoring network only consisted of one permanent radial tiltmeter (south of Bory crater) and one permanent extensometer located in Bory crater (Fig. 2a). Data from these stations were telemetered to the observatory every five minutes. In addition, twenty-five spirit-level tilt (dry-tilt) stations and a levelling network were frequently measured.

The monitoring network has been progressively improved and in 2007 it included 8 continuous tiltmeters, 4 continuous extensometers (equipped with extension, vertical and shearing components) and 12 continuous GPS stations (Fig. 2b). These permanent stations record ground displacements at 30 s to 60 s intervals. In addition, a network of 80 stainless steel benchmarks is surveyed by GPS campaigns immediately after each eruption.

For more information on deformation monitoring results at Piton de La Fournaise, see Delorme et al. (1989), Lénat et al. (1989a,b), Toutain et al. (1992), Battaglia and Bachèlery (2003) and Peltier et al. (2005, 2006, 2007, 2008).

3. The 1972–1992 period of activity

3.1. Eruptive activity

Following six years of repose, eruptive activity began at Piton de La Fournaise in June 1972 with four successive eruptions in less than six months on the northern, southern and eastern flanks (Krafft and Gerente, 1977). Over the next 20 years, 36 additional eruptions and 5 intrusions followed (Fig. 1c; Table 1). Most of the activity, except the 1977 and 1986 eruptions, took place within the Enclos Fouqué caldera, mainly along the rift zones or inside the Dolomieu crater (Fig. 1c). Distal eruptions located outside of the Enclos Fouqué caldera occurred in 1977 and 1986 (Fig. 3a). In April 1977, an eruptive fissure opened in the eastern part of Dolomieu crater before propagating across La Plaine des Osmondes and extending outside of the Enclos Fouqué along the NE rift zone (Fig. 1c; Table 1; Kieffer et al., 1977). In March–April 1986, eruptive fissures opened along the SE rift zone, first inside and then outside the Enclos Fouqué caldera (Fig. 1c; Table 1; Delorme et al., 1989). The largest volumes of lava were produced during these distal eruptions, with 20×10^6 m³ in April 1977 (re-evaluated after Delorme, 1994) and 14×10^6 m³ in March–April 1986 (Delorme et al., 1989) compared to a mean of 4×10^6 m³ for the proximal eruptions and less than 2×10^6 m³ for the eruptions restricted to the Dolomieu crater (Fig. 3b; Table 1).

Few morphological changes occurred in the summit craters between 1972 and 1992. Several summit eruptions (May 1973, November 1975, April 1977, September and December 1985, July, November and December 1986, June 1987, January 1990, August 1992,

Table 1) filled the Dolomieu crater with lava to a depth of 20–30 m. In 1986, a pit-crater (80 m deep and 150 m in diameter, Delorme et al., 1989) formed in the eastern part of the Dolomieu crater just after the 1986 distal eruption.

3.2. Geophysical recordings

3.2.1. Inter-eruptive behaviour

Since the establishment of the OVPF in 1980, seismic and deformation data have been recorded continuously. The 1981–1992 eruptions were investigated in several publications (Bachèlery et al., 1982; Delorme et al., 1989; Lénat et al., 1989a,b; Zlotnicki et al., 1990; Cayol and Cornet, 1998). Between a few days and three weeks prior to eruption a slight increase in seismicity located between 1 and 3 km below the summit craters was recorded. This pre-eruptive seismicity was limited to about five to ten volcano-tectonic events per (Lénat and Bachèlery, 1987). Following the July 1985 intrusion and before the 1986 distal eruption, volcano-tectonic earthquakes were also recorded on the eastern flank, about 3–6 km from the summit, at around 4–7 km depth (Lénat et al., 1989a).

Except for the 1985–1986 eruptions, no significant ground deformation accompanied the pre-eruptive seismicity recorded during the days or the weeks prior to an eruption. By contrast the 1985–1986 eruptions were preceded by several months of summit inflation (Lénat and Bachèlery, 1987). This deformation was limited to the summit and reached up to 50 μ rad on the BORi station (Lénat et al., 1989a). After the March–April 1986 eruption, and just before the pit-crater formation, a progressive summit deflation was recorded. The deflation source was estimated to 0.1–0.4 km depth using a point source model (Delorme et al., 1989). A slow summit deflation ($2\text{--}3 \mu\text{rad month}^{-1}$) had also been measured in the summit area after the 1981 and 1984 eruptions (Lénat et al., 1989a,b).

3.2.2. Syn-eruptive behaviour

Continuous geophysical data recorded since 1980 reveal a recurrent eruptive pattern (Bachèlery et al., 1982; Delorme et al., 1989; Lénat et al., 1989a,b; Lénat and Bachèlery, 1990; Toutain et al., 1992). A few minutes or hours before each eruption, a volcano-tectonic seismic swarm began and was accompanied by rapid summit inflation reaching up to several hundred microradians of tilt and up to 50 cm vertical motion at the summit. The focus of the seismic swarm, located at a depth of 1 to 2 km below the Dolomieu crater, differed slightly from one eruption to the next (Lénat and Bachèlery, 1990), but in each case an upward magma migration below the Dolomieu crater was observed and was followed by a lateral migration towards one of the volcano flanks for the proximal and distal eruptions (Toutain et al., 1992).

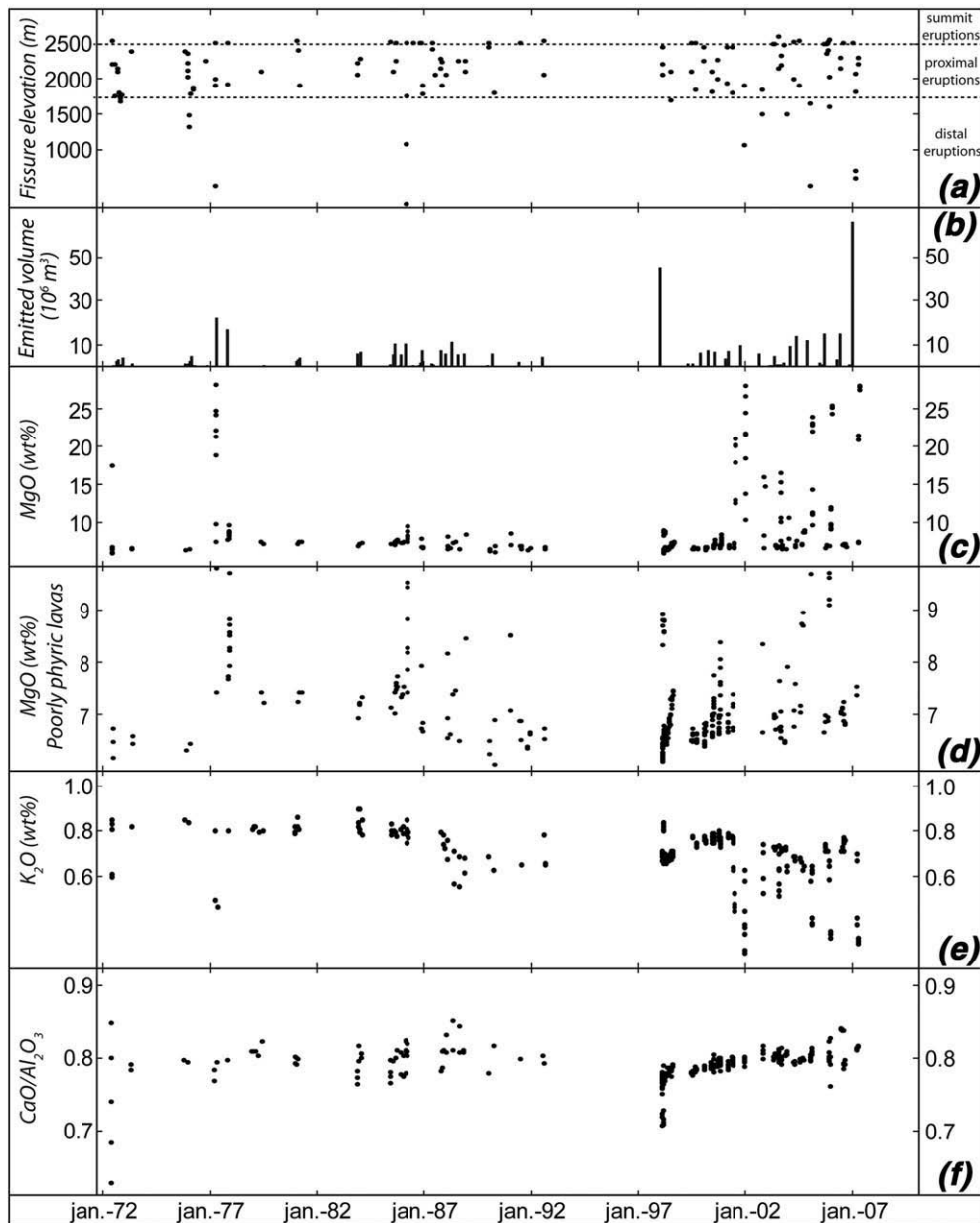


Fig. 3. Time series plots for eruptions during 1972–2007 giving (a) the highest and the lowest elevations of each fissure, (b) emitted volume of lava flows, (c) MgO (wt%) concentration in erupted lavas, (d) MgO (wt%) concentration in only poorly phyrlic lavas, (e) K_2O (wt%) concentration in erupted lavas, and (f) CaO/Al_2O_3 ratio in erupted lavas. Geochemical data are from Boivin and Bachèlery, 2009–this issue, Peltier (2007), Vlastélic et al. (2007).

For the 1972–1992 period, only the dyke feeding the 1983–1984 eruption has been modelled, using photogrammetric data (Zlotnicki et al., 1990; Cayol and Cornet, 1998). Using a simple half-space model (Okada, 1985), Zlotnicki et al. (1990) explained the observed ground deformation as being due to a 65° dipping dyke, originating below the Dolomieu crater at a depth of about 3 km (which corresponds to the bottom of the seismic swarm), and connected to two quasi-vertical dykes (dipping 81° and 86°). Conversely, using a 3D mixed boundary element method, Cayol and Cornet's model consisted of a 45° dipping dyke, originating at a depth of 1.5 km (i.e. the top of the seismic swarm) (Cayol and Cornet, 1998).

4. The 1998–2007 period of activity

4.1. Eruptive activity

After six years of repose, on March 6, 1998, a seismic swarm migrated from a depth of 7.5 km to the surface leading to the opening of eruptive

fissures on March 9 (Battaglia et al., 2005). It was the first time since the implantation of the observatory that such a deep seismic migration had been observed at Piton de La Fournaise. Three days after the opening of the first eruptive fissures on the northern flank (March 9 – Piton Kapor), a new fissure opened on the western flank (March 12 – Hudson crater). The eruption continued until September 1998.

Following this unusually long eruption (196 days), twenty-four eruptions and one intrusion occurred until 2007 (Table 1). Between 1998 and 2001, the eruptions were only proximal along the N25–30 and the N120 rift-zones (Fig. 1c) and emitted moderate volumes of lava, usually less than $10 \times 10^6 \text{ m}^3$ (Figs. 3a, b and 4a and Table 1). From 2000, eruptive activity can be defined by cycles that began with summit or proximal eruptions and ended with a distal eruption (Fig. 4a). Of the five distal eruptions to have occurred during 2002–2007, four took place in La Plaine des Osmondes (January 2002, January 2004, February 2005 and December 2005, Table 1) and one was on the south-eastern flank at an elevation of 600 m (April 2007).

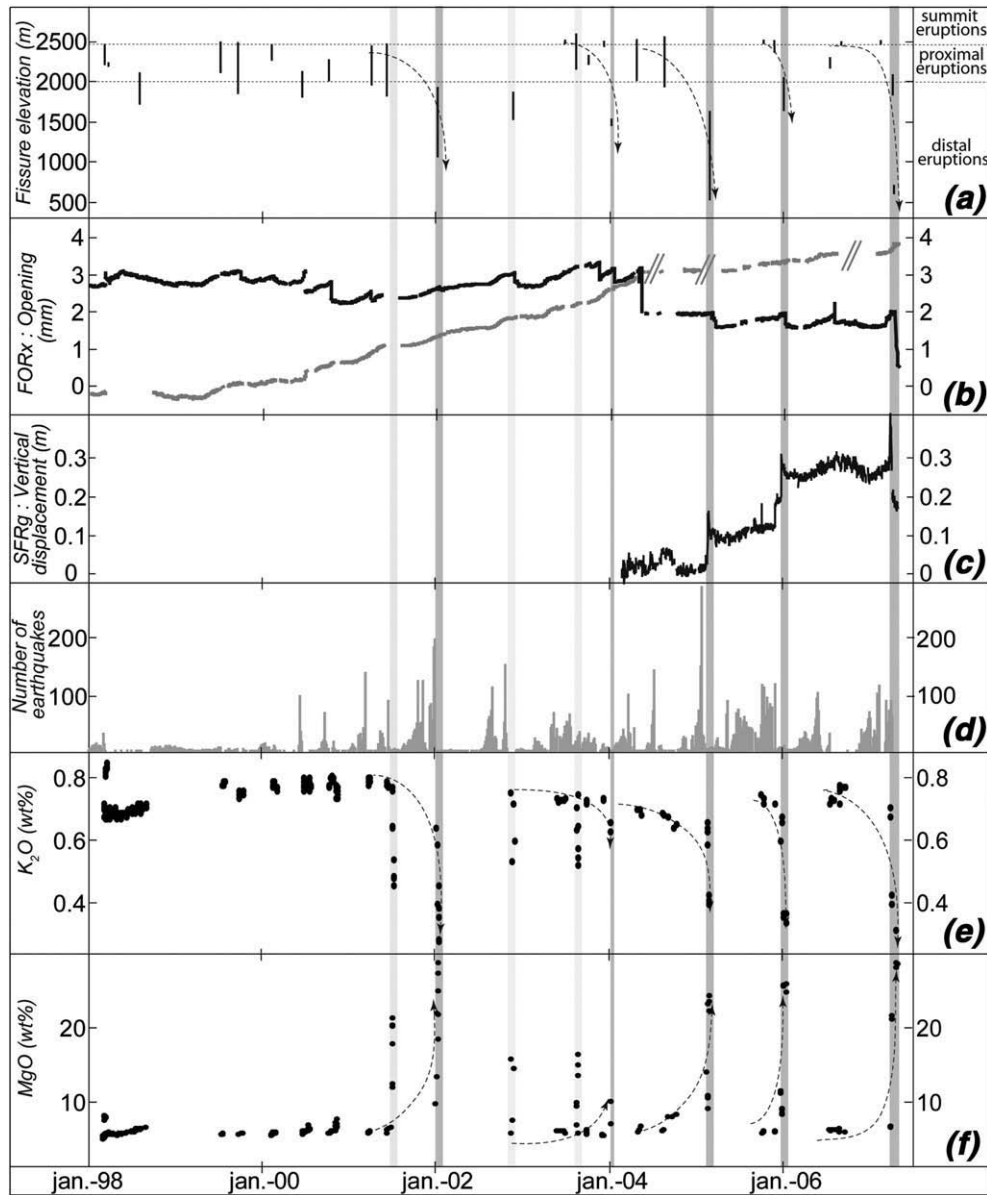


Fig. 4. Time series plots of the 1998–2007 eruptive period giving (a) fissure elevation, (b) opening of the FORx fracture recorded by an extensometer, with (black) and without (grey) rapid displacements linked to the emplacement of dyke, (c) vertical displacement of the SFRg GPS benchmark, (d) daily number of earthquakes, (e) K_2O (wt.%) in erupted lavas, and (f) MgO (wt.%) in erupted lavas. Geochemical data are from Peltier (2007), Vlastélic et al. (2005) and Vlastélic et al. (2007). Shaded areas represent oceanite (dark grey) and olivine-rich (light grey) eruptions and the dotted arrows represent the cycles defined in the text.

Similar to the 1972–1992 eruptive period, the distal eruptions emitted the largest volumes of lava, averaging $20 \times 10^6 \text{ m}^3$ with a maximum value of $110\text{--}140 \times 10^6 \text{ m}^3$ for the April 2007 eruption (Michon et al., 2007b; Staudacher et al., 2009-this issue). The mean value for the proximal and summit eruptions was $7 \times 10^6 \text{ m}^3$ and $1.5 \times 10^6 \text{ m}^3$, respectively (Fig. 3b; Table 1). Two exceptions to this generalization are the January 2004 distal eruption, which lasted only one day and emitted less than $2 \times 10^6 \text{ m}^3$ of lava even if $7.5 \times 10^6 \text{ m}^3$ of magma have been estimated to be involved in the dyke from inversion of interferometric data (Tinard, 2007); and the August 2006–January 2007 summit eruption, which emitted around $18 \times 10^6 \text{ m}^3$ of lava (nine times larger than the average for summit eruptions).

During 1998–2007, about $334 \times 10^6 \text{ m}^3$ of lavas were erupted, compared to about $230 \times 10^6 \text{ m}^3$ for the 1972–1992 period (Table 1). The 1998–2007 period also saw 20–30 m of lava flow accumulation in the Dolomieu crater, which led to overflows on the eastern margin of the crater during the August 2006–January 2007 and February 2007

eruptions. Two collapses also occurred in the Dolomieu crater during the 1998–2007 period. In December 2002, a pit-crater formed in the southwestern part of the Dolomieu crater (20 m deep and 200 m in diameter; Longpré et al., 2007), and in April 2007, the whole floor of the Dolomieu crater collapsed (340 m deep; Michon et al., 2007b; Staudacher et al., 2009-this issue).

4.2. Geophysical recordings

4.2.1. Inter-eruptive behaviour

Between 1992 and 1998, no eruptive activity was observed (Fig. 3a, b). From 1992 to 1996, GPS displacements indicated minor summit deflation (around 1 cm y^{-1}) probably due to thermal contraction of shallowly stored magma (Briole et al., 1998). In September 1996, a seismic swarm occurred in the northern part of La Plaine des Sables (~6 km northwest of the summit cone, Fig. 1c) with thirty-six events located at a depth of 15 km (Valérie Ferrazzini-OVPE, personal communication). After this

deep seismic swarm, an intrusion, not followed by an eruption, occurred in November 1996 at about 2 km depth below the northern flank of the volcano (Bachèlery, 1999). After the November 1996 intrusion, slight summit inflation ($10 \mu\text{rad y}^{-1}$ at TCRI station, Bachèlery, 1999) and an increase of the shallow seismicity began.

The FORx extensometer station operated during the entire 1998–2007 eruptive period (Fig. 4b). Data from 1998–2003 were described by Peltier et al. (2006), and reveal that the fracture monitored by the FORx extensometers began to open 1 to 5 months before each eruption (Fig. 4b). The fracture experienced months-long periods of no change after the eruptions of June 2001, January 2002, November 2002, August 2004, February 2005, December 2005 and April 2007, which emitted the largest volumes of lava (Fig. 3b; Table 1). The systematic fracture opening before eruptions has been attributed to volcano dilatation in response to the inflation of the cone. In contrast to the 1980–1992 period, summit inflation was observed in the weeks and months prior to each eruption occurring between 2000 and 2007, with surface displacements reaching up to 10 cm (Figs. 4c and 5; Peltier et al., 2007, 2008). From 2000 to 2007, summit inflation was continuous and only interrupted by deformation due to dyke injections, eruptions and post-eruptive summit deflation that followed large-volume distal eruptions (Fig. 4c).

The character of pre-eruptive summit inflation was similar from one eruption to the next and is attributed to a pressurized magma reservoir located at a depth of around 2300 m below the summit craters (Peltier et al., 2007, 2008), just below the pre-eruptive seismic swarms (Fig. 5; Nercessian et al., 1996). From 2000 to 2007, pre-eruptive summit inflation was accompanied by an exponential increase of the seismicity, reaching more than one hundred events per day, whereas between 1998 and 2000 the pre-eruptive seismicity was limited to about twenty events per day (Fig. 4d). The majority of earthquakes were volcano-tectonic events located 500–2500 m below

the Dolomieu crater. On April 2005 and April 2007, volcano-tectonic earthquakes located at a depth of 7.5 km were also recorded west of the Bory crater (Valérie Ferrazzini-OVPF, personal communication).

4.2.2. Syn-eruptive behaviour

Similar to 1972–1992, all dyke injections were accompanied by significant ground deformation and by seismic swarms (generally several hundred volcano-tectonic earthquakes with $M < 2$, located between 500 to 2500 m depth). The strong seismic and ground deformation activity usually occurred 15 min to several hours before eruptions (Fig. 4b, d). During intrusive activity that culminated in distal eruptions (January 2002, January 2004, February 2005, December 2005, and April 2007), and in November 2002 volcano-tectonic events were also recorded on the eastern flank of the volcano at a depth of 2.5–5 km.

Dynamics of dyke propagation during the 1998–2007 period were studied by Peltier et al. (2005) using tiltmeter and seismic background noise data and by Peltier et al. (2007, 2008) using GPS data. These studies revealed two stages in the dyke propagation: vertical migration from the magma reservoir located below the Dolomieu crater (10 to 50 min) followed by lateral migration towards the flank of the volcano for the proximal and distal eruptions (10 min to several hours). For distal eruptions, the vertical magma migration lasted for only a few minutes (Peltier et al., 2008). Displacements recorded by GPS associated with each eruption suggested the existence of two preferential vertical feeding pathways below the Dolomieu crater (Peltier et al., 2007, 2008). Dykes feeding proximal and distal eruptions originated below the western and the eastern part of the Dolomieu crater, respectively (Fig. 6).

3D mixed boundary element models (Cayol and Cornet, 1998) of GPS and tiltmeter data associated with the 2003–2005 eruptions, indicate that the depth of dyke initiation varied according to eruptive

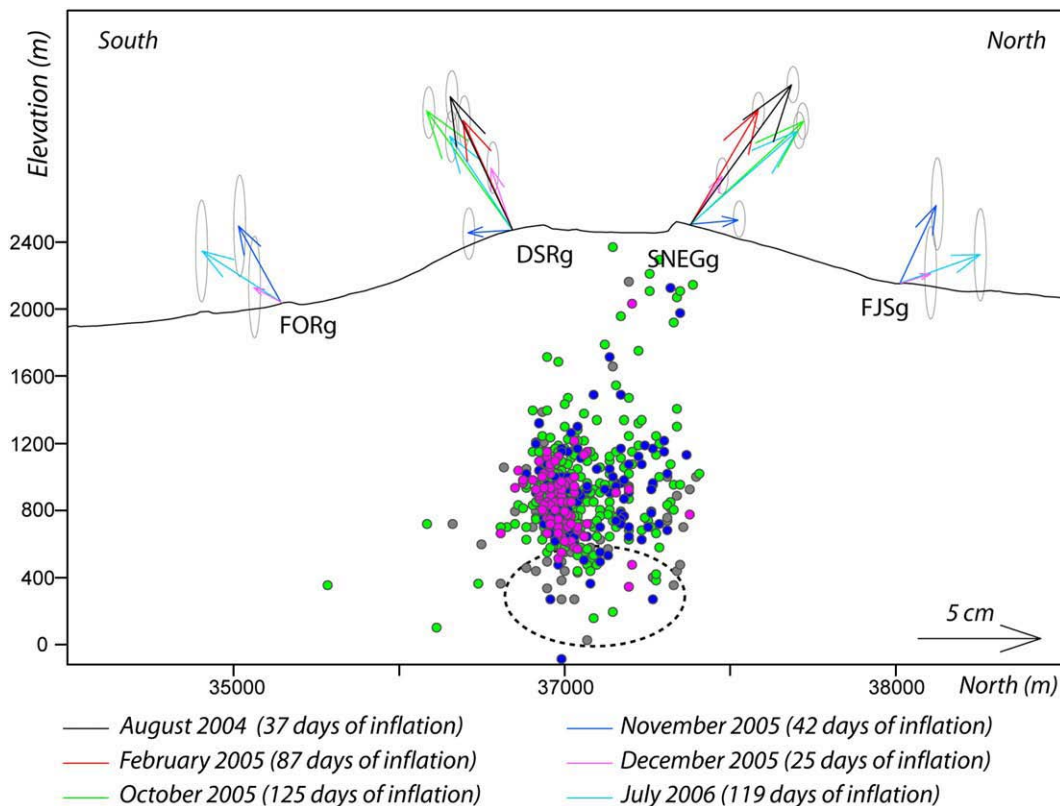


Fig. 5. North-south cross section through Piton de La Fournaise with pre-eruptive GPS displacements recorded before the August 2004, February 2005, October 2005, November 2005, December 2005 and July 2006 eruptions. Coloured circles correspond to hypocenters of the pre-eruptive seismic swarms associated with the listed inflation periods (Valérie Ferrazzini-OVPF, personal communication). Dotted circle represents the location of the modelled magma reservoir after Peltier et al. (2008) (Gauss Laborde Réunion coordinates, meters).

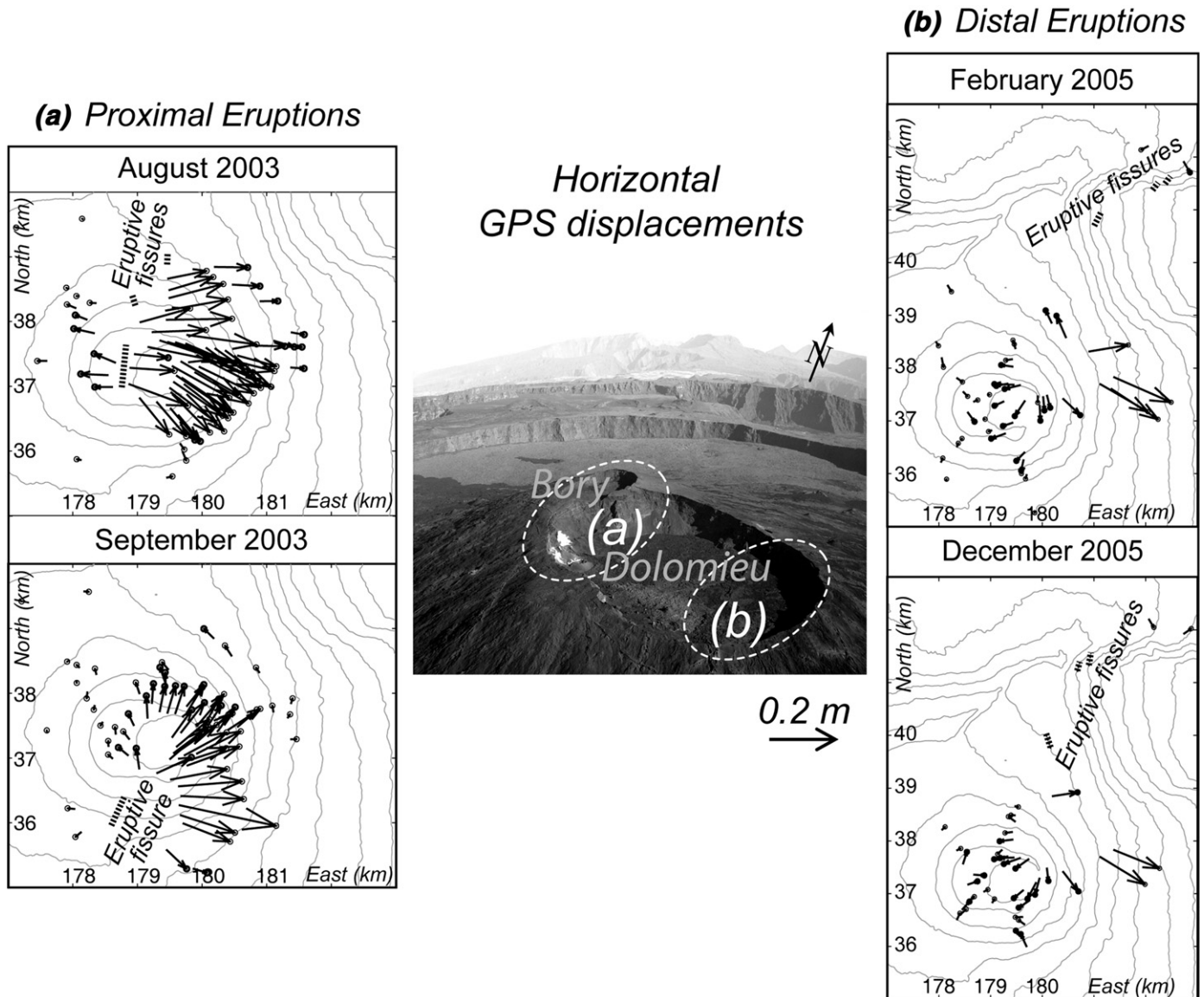


Fig. 6. Examples of horizontal displacements (from GPS) caused by dyke injections associated with (a) proximal eruptions (examples from August and September 2003 eruptions) and (b) distal eruptions (examples from February and December 2005 eruptions). Dotted white circles represent the source areas for the dykes leading to (a) proximal and (b) distal eruptions.

fissure location (Peltier et al., 2008). Dykes feeding summit eruptions started at shallower depths (1700–2000 m) than those feeding distal eruptions (~2200–2300 m; Peltier et al., 2008). Numerical models of InSAR data associated with the 1998–2006 proximal eruptions, and using the same 3D mixed boundary element method (Cayol and Cornet, 1997), suggest shallower dykes (<1500 m deep) dipping 53°–75° (Froger et al., 2004; Fukushima, 2005; Fukushima et al., 2005; Tinard, 2007). Sigmundsson et al. (1999) and Battaglia and Bachèlery (2003), using a simple half-space model (Okada, 1985), explained also interferometric (Sigmundsson et al., 1999) and tiltmeter (Battaglia and Bachèlery, 2003) data associated with the 1998 eruption by a shallow dyke (around 1000–1500 m deep).

5. Petrological and geochemical data (1972–2007)

5.1. Petrological composition

With the exception of the lavas erupted in March 1998 (Hudson crater), lavas emitted between 1972 and 2007 can be petrographically divided into three groups according to the location of the eruptive

fissures (Table 1): (1) poorly phyric lavas (SSB type) with less than 5% phenocrysts consisting of small olivine (Fo_{80-76}), clinopyroxene and plagioclase crystals, were emitted during summit eruptions and during the September 2003 proximal eruption; (2) poorly phyric lavas (SSB type) with less than 5% phenocrysts consisting only of small olivine (Fo_{84-78}) and clinopyroxene, not accompanied by plagioclase, characterised most of the proximal eruptions; (3) Olivine-rich basalts (10–20% olivine crystals) and oceanites (more than 20% olivine crystals), were erupted during the proximal and distal eruptions of November–December 1972, April 1977, October–November 1977, June 2001, January 2002, November 2002, August 2003, January 2004, February 2005 and December 2005. The third type of lavas was emitted during high effusion rate eruptions (Fig. 7). The modal increase of olivine macrocrysts (and thus MgO wt.%) occurred at the end of a few eruptions when a significant increase in RSAM (Real-Time Seismic Amplitude), corresponding in surface to an increase of the effusion rate, was recorded (Fig. 7). Olivine crystals from these lavas have higher $Fo\%$ values (Fo_{86-81} with an average of Fo_{84} for the 1972–2007 lavas, Peltier, 2007; Boivin and Bachèlery, 2009-this issue). The highest olivine content (40–50%) was found in lavas erupted outside of

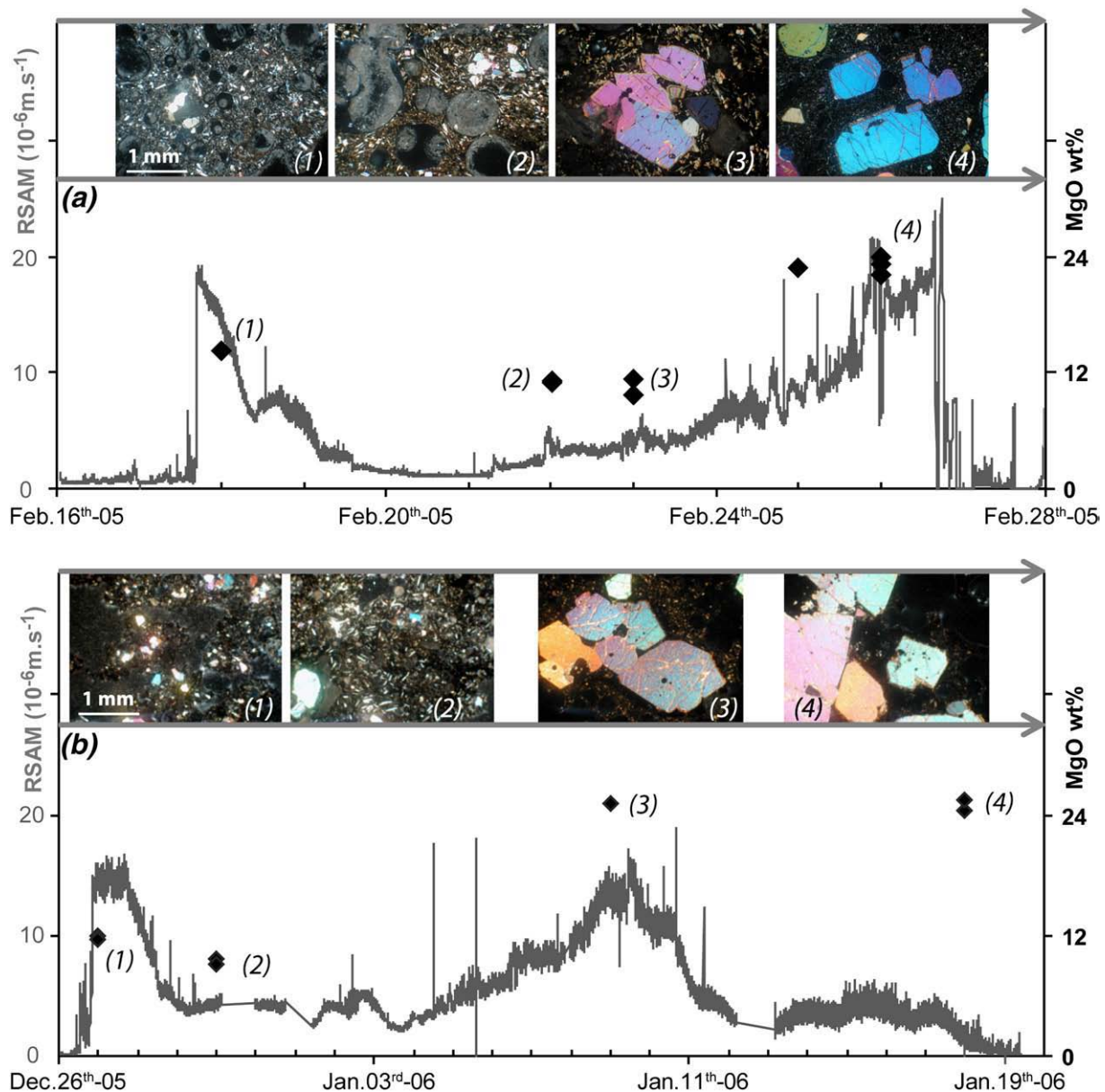


Fig. 7. Comparison between the RSAM (Real-Time Seismic Amplitude, noted by curves below photomicrographs) recorded on the seismic station NSR (see Fig. 2 for location), MgO weight percent (black diamonds), and mineral composition (photomicrographs) of erupted lavas during the (a) February 2005 and (b) December 2005–January 2006 distal eruptions. On the MgO plot, numbers refer to the corresponding photomicrographs.

the summit cone in the lower parts of the volcano (in January 2002, February 2005 and April 2007).

5.2. Major element composition

Between 1972 and 2007, the bulk compositions of the lavas were relatively homogenous, except for fluctuations due to variable olivine crystal content (Fig. 3c, e, f). The frequent occurrence of olivine-rich lavas pushes the MgO wt.% composition trend towards high MgO values, ranging from 9.7 to 14.4 wt.% for olivine-rich basalts and from 17 to 28 wt.% for oceanites. Poorly phryic SSB lavas show minor variation in MgO wt.%, typically between 6.5 and 7.5 wt.%. However, MgO wt.% values generally decreased between 1977 and 1992, and increased during 1998–2007, even if considering only the poorly phryic lavas (Fig. 3c, d). The increase of MgO in poorly phryic lavas erupted between 1998 and 2007, suggests increasing influence of a more primitive magma over time, whereas the peak of MgO wt.% in

oceanitic lavas strongly relates to the modal content of olivine macrocrysts (Figs. 3c and 7; Albarède and Tamagnan, 1988).

At the beginning of both the 1972–1992 and 1998–2007 eruptive periods, the $\text{CaO}/\text{Al}_2\text{O}_3$ ratio displayed the largest range of values (Fig. 3f). After 1972, the ratio remained stable at around 0.79–0.80. Despite some fluctuations, no long-term trend is apparent for this period. Between 1998 and 2007, the $\text{CaO}/\text{Al}_2\text{O}_3$ ratio increased steadily from 0.77 to 0.81 and reached the highest value for post-1931 lavas of 0.84 in 2005 (Albarède and Tamagnan, 1988).

Potassium, as an incompatible element with respect to the Piton de La Fournaise crystallizing assemblage, is a good indicator of the origin of basaltic liquid. With exception of dilution effects due to accumulation of olivine xenocrysts, variations in potassium may be attributed to variations in mantle source composition, degree of melting of a single source, or assimilation of crustal material. The drop in the K_2O wt.% in 1988 distinguishes two geochemical periods between 1972 and 1992 (Fig. 3e, Boivin and Bachèlery, 2009–this issue). Basalts erupted between

1977 and 1987 contained an average of 0.81% K_2O , whereas the lavas erupted between 1988 and 1992 contained an average of 0.6 to 0.7% (Fig. 3e). The decrease in K_2O observed in 1988, which did not correlate with any change in MgO wt.%, is interpreted as the coexistence of at least two magma batches in the shallow storage complex of the volcano at this time (Boivin and Bachèlery, 2009-this issue).

The March 1998 eruption emitted two distinct types of lava. On March 9, 1998, a fissure opened on the northern flank (Kapor) emitting SSB lavas, and on March 12, 1998, a second fissure opened on the western flank (Hudson) emitting more magnesian lavas (AbG) until April 1, 1998 (Fig. 4e, f). Bureau et al. (1999) suggested a deeper origin for the Hudson lava. The later 1999–2001 lavas were homogeneous and poorly-phyric and were similar to the Kapor lavas with only slight K_2O and MgO content variations (Figs. 3c, e, f and 4e, f). Between 1998 and 2001, the K_2O content increased slightly, and then decreased after 2001. Since 2001, the K_2O content changed after each oceanite eruption, allowing definition of five geochemical cycles: end of 2000–January 2002, November 2002–January 2004, May 2004–February 2005, October 2005–December 2005 and July 2006–April 2007 (Fig. 4e, f). Each cycle began with a summit or proximal eruption that erupted poorly phyric lavas and ended with a distal eruption of oceanite lavas. During a cycle, the first lavas of each eruption, depleted in olivine macrocrysts, displayed a progressive rise in compatibles (like MgO, Fig. 4f) and a corresponding depletion in incompatibles (like K_2O , Fig. 4e). This behaviour suggests the influence of increasingly primitive magmas during the course of an individual cycle, as already mentioned by Peltier et al. (2008) for the 2004 and 2005 cycles (Fig. 3d).

6. Discussion

Evolution of eruptive style, ground deformation, pre-eruptive seismicity and lava compositions over time highlights fundamental changes in the behaviour of Piton de La Fournaise volcano during 1972–2007. Data collected by OVPF since 1980, allow us to propose a model for magma transport and storage during the monitored period.

6.1. Evolution of eruption triggering processes

The large range of CaO/Al_2O_3 values for the 1972 and 1998 lavas suggests the involvement of different magmas at the beginning of the two eruptive sequences. Albarède et al. (1997) propose from trace elements study that CaO/Al_2O_3 variations at Piton de la Fournaise are mostly related to clinopyroxene fractionation. For the 1998–2006 lavas, Vlastélic et al. (2007) suggests also a pyroxene control to explain the negative correlation between the CaO/Al_2O_3 ratio and the Fe_2O_3/MgO ratio for aphyric samples. Evidence of clinopyroxene accumulation was only mentioned in ultramafic autoliths by Upton and Wadsworth (1972), so given the lack of evidence for pyroxene accumulation in the 1972–2007 lavas, an increase in CaO/Al_2O_3 is indicative of a less clinopyroxene-fractionated magma. In the case of the 1972 and 1998 activity, we propose that at least two distinct magmas fed these eruptions, one that is residual melt and had undergone 6 years of fractionation, and a second that was more primitive. In 1998, the resumption of activity was preceded by deep seismicity (7.5 to 2.5 km depth), indicating the arrival of new magma into the shallow reservoir (Battaglia et al., 2005). Because there was no instrumentation on the volcano in 1972, we have no clear evidence of recharging prior to the 1972–1992 eruptive period; however, similarities between the 1972 and 1998 eruptions suggest that such recharging may have occurred before the 1972 eruptions.

Between 1972 and 2007, two main pre-eruptive patterns are suggested by geophysical data. The 1981 to 1992 (no geophysical data available between 1972 and 1981) and the 1998 to 2000 eruptions were mostly preceded by days of low-level seismicity (about ten volcano-

tectonic earthquakes per day), whereas the 2001 to 2007 eruptions were preceded by weeks to months of strong seismic precursors (about one hundred volcano-tectonic earthquakes per day) and summit inflation. These two distinct types of precursors suggest a change in the magmatic system of Piton de La Fournaise in 2000, and thus an evolution in the eruption triggering processes.

6.1.1. 1980–1992 and 1998–2000: weak geophysical eruptive precursors

Between 1972 and 2000, all eruptions (except the November–December 1972, April 1977 and March–April 1986 eruptions) were at the summit or close to the summit and emitted low volumes of poorly phyric lavas with homogeneous bulk compositions. According to Lénat et al. (1989a, b) and Boivin and Bachèlery (2009-this issue), the 1979, 1981, 1983–1984, and June 1985 lavas could be derived from the same batch of magma as the October–November 1977 lavas by fractional crystallization of a gabbroic cumulate (Fig. 3c, d, e, f). The 1979 to 1985 lavas are therefore interpreted as having been fed by successive inputs from the same batch of magma evolving at low pressure since at least 1977 (Delorme et al., 1989; Lénat et al., 1989a, b; Albarède, 1993). The high eruptive frequency and the small volume of lavas erupted during each effusive episode during this period reveal that failure of the reservoir and dyke formation may be induced by low magma overpressures due to crystallization processes (Tait et al., 1989).

The absence of significant summit inflation prior to the 1981–1985 eruptions and the slight decrease of the MgO wt.% content observed in the lavas emitted over this period (Fig. 3d) lead us to speculate that the shallow magma reservoir was not regularly recharged between 1972 and 1992. November–December 1972 and April 1977 oceanite lavas could be indicative of shallow reservoir recharging (Bachèlery, 1981; Albarède and Tamagnan, 1988) but without geophysical data, however, we cannot test the geochemically-based recharging hypothesis. The 1986 distal eruption, preceded by one year of slight pre-eruptive summit inflation and seismicity located 4–7 km below the volcano's eastern flank, could also highlighted a deep recharge of the shallow reservoir as shown by the high eruption frequency from 1986 to 1988 and the evolution of the Pb isotopic compositions. Variations of Pb isotopic compositions observed during the March 1986 eruption are interpreted as resulting from mixing between magmas already residing in the shallow plumbing system and deeper melts that have not interacted with crustal component (Vlastélic et al., 2009-this issue). The lavas erupted in March–April 1986 differed slightly from the 1979 to 1985 lavas mostly by their higher olivine (up to 4%) and MgO content (7.8 to 9.5 wt.%, Fig. 3c, d). The K_2O drop in 1988, attributed to the involvement of a different magma batch derived from the same mantle source as other Piton de La Fournaise magmas (Boivin and Bachèlery, 2009-this issue), could result from the recharge of the magma reservoir in 1986.

As previously mentioned, deep seismic activity (7.5 to 2.5 km depth) and magmas compositions of the March to September 1998 eruptions clearly indicate the arrival of new magma into the shallow reservoir. Between 1998 and 2000, lava compositions and the lack of significant geophysical eruptive precursors indicate that the shallow plumbing system was not being recharged. The lava compositions may be explained in terms of mixing between the two end-members erupted in 1998, Kapor and Hudson, (Bachèlery, 1999) and progressive contamination by host rock (Vlastélic et al., 2005).

6.1.2. 2000–2007: strong geophysical eruptive precursors

The pattern of eruptive behaviour that characterized Piton de La Fournaise since 1972 was disturbed in 2000 with the appearance of strong geophysical precursors that occurred weeks to months prior to eruptions. Eruptions also tended to group into cycles characterized by: (1) decreasing elevation of the eruptive vents (most of cycles began with summit or proximal eruptions and ended with a distal eruption), (2) dyke roots that deepened over time, (3) increase in

MgO content of erupted lavas over time, (4) summit inflation throughout the cycle (5) slight deflation at the end of each cycle.

According to these criteria, five cycles were defined (Fig. 4a, e, f): (1) end of 2000–January 2002 (4 eruptions), (2) November 2002–January 2004 (5 eruptions and 1 intrusion), (3) May 2004–February 2005 (3 eruptions), (4) October 2005–December 2005 (3 eruptions), and (5) July 2006–April 2007 (4 eruptions).

6.1.2.1. Origin of continuous inflation. According to ground deformation and seismic data (Peltier et al., 2007; Brenguier et al., 2008) no shallow magma intrusion towards the surface occurred between eruptions during 2000–2007. Pre-eruptive summit inflation was attributed to an overpressurized magma reservoir located at a depth of about 2300 m (Peltier et al., 2007, 2008). Overpressure in the reservoir can be generated by magma recharge (Blake, 1981) or crystallization (Tait et al., 1989). Evolution of lava composition towards MgO-rich poorly phyric lavas over a same cycle and the lack of phenocrysts argue against crystallization mechanisms. We therefore propose that the nearly constant summit inflation after 2000 was caused by quasi-continuous recharging of the shallow magma reservoir. Continuous recharge of the shallow magma reservoir explains the high volume emitted since 1998, $334 \times 10^6 \text{ m}^3$ in 10 years, compared to $230 \times 10^6 \text{ m}^3$ emitted in 20 years between 1972 and 1992. According to the Pb isotope studies (Vlastélic et al., 2007), the whole system (from the oceanic crust to the shallow reservoir) has been also recharged by a new magma in 2005.

6.1.2.2. Origin of eruptive sequences during a cycle. Cycles that include multiple eruptions begin with low-levels of eruptive activity (summit or proximal eruptions characterized by low effusion rate and low erupted volumes, $< 3 \times 10^6 \text{ m}^3$). Concentration of activity in the summit area confirms the presence of a pressurized magma reservoir beneath

the summit. At the beginning of an eruptive cycle, the volcano is in a state of structural stability and rupture of the shallow magma reservoir tends to occur at the top, where the lithostatic pressure is the lowest. At Piton de La Fournaise, this implies that magma will rise to the summit of the volcano from a source beneath the western part of the Dolomieu crater, leading to summit or proximal eruption (Figs. 6 and 8; Mériaux, 1996; Pinel and Jaupart, 2004). Summit inflation restarted immediately after each summit or proximal eruption, indicating continued recharge of the shallow reservoir.

At Etna volcano, Allard et al. (2006) suggested that continuous recharging of the magma reservoir can pressurize and destabilize the unbuttressed eastern flank of the edifice, which facilitates eruptions on the eastern flank. At Piton de La Fournaise, structural analyses and geodetic measurements have shown that the eastern part of the central cone was affected by an eastward motion (Bachèlery, 1981; Delorme et al., 1989; Lénat et al., 1989a,b,c; Zlotnicki et al., 1990; Briole et al., 1998; Sigmundsson et al., 1999; Froger et al., 2004; Fukushima et al., 2005; Carter et al., 2007; Peltier et al., 2007). The flank instability can be explained by stress accumulation on the unbuttressed eastern flank due to the successive intrusion and accumulation of magma in the reservoir. The preferential motion of the eastern flank was especially well visible during the large distal eruption of April 2007. Interferometric data reveal a motion of up to 80 cm of the eastern flank towards the sea (Augier et al., 2008). Motion of the eastern flank (Duffield et al., 1982; Lénat et al., 1989c) may be partly due to creep facilitated by the rheidity of the olivine-cumulates within the structure as proposed by Clague and Denlinger (1994) for Kilauea Volcano. Dislocation lamellae sometimes observed in olivine crystals of the oceanites could be generated by such solid-state gravitational creep and slumping towards the unsupported eastern flank of the volcanic edifice as proposed by Upton et al. (2000). Seismic swarms recorded before and during major distal eruptions at depths of 4–7 km below the eastern flank of Piton de La Fournaise may

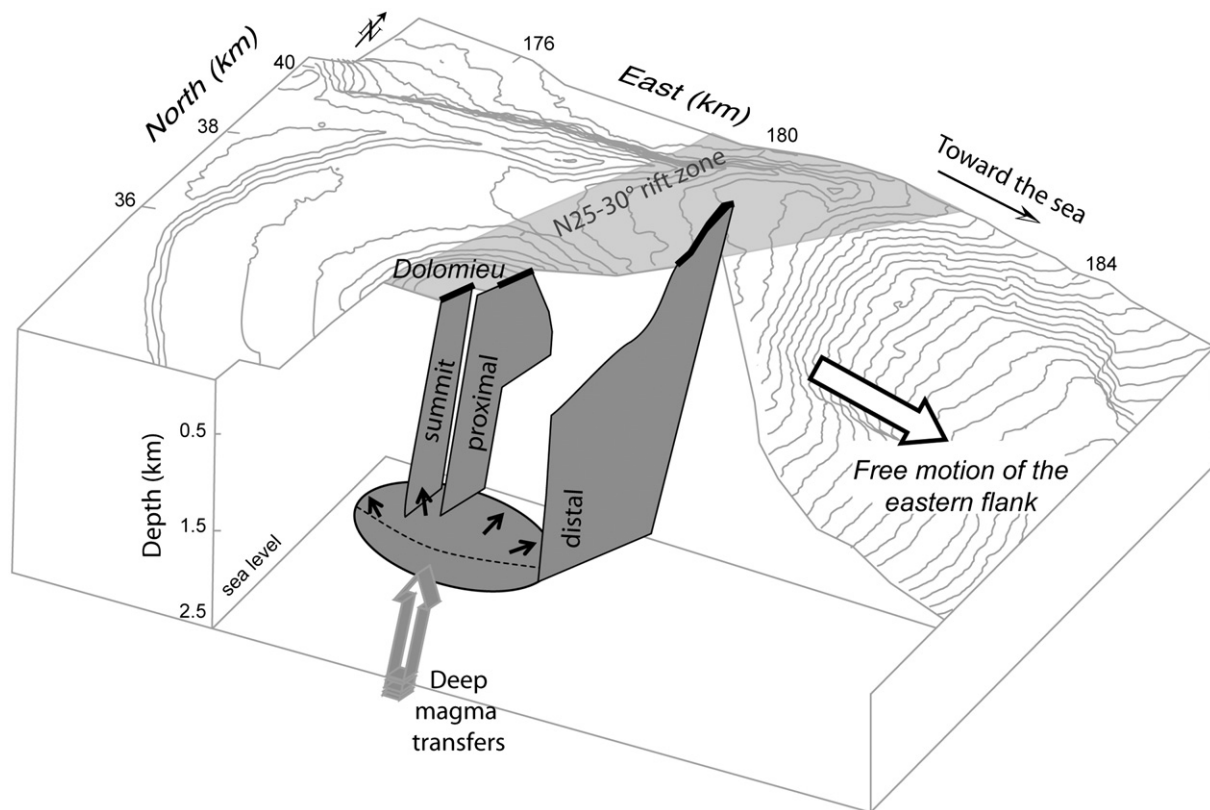


Fig. 8. Schematic model of the shallow magmatic system of Piton de La Fournaise. Dykes feeding the summit and proximal eruptions started at the top of the shallow reservoir, whereas the dykes feeding the distal eruptions started at the base and eastern part of the magma reservoir. The bold lines represent eruptive fissure locations. The shaded grey area shows the N25–35° rift zone extension in surface.

indicate fracture reactivation possibly linked to the eastern flank instability. By contrast, Upton et al. (2000) explained the seismic swarms at 4–7 km depth by the presence of a magma reservoir at this level extending up to the eastern flank but lack of deformation signal starting from the east during magma injections avoid us to validate this explanation.

Distal eruptions are characterized by high effusion rates ($10\text{--}20\text{ m}^3\text{ s}^{-1}$) and high olivine content (commonly $>40\%$). Rapid magma migration allows the incorporation of olivine macrocrysts, extracted from underlying dunitic complexes, from the walls of the magma reservoir or from olivine-enriched liquid stored at the base of the magma reservoir. The influence of the high effusion rate on olivine incorporation can be highlighted by the strong correlation observed between the increase of MgO content and the increase of effusion rate (related to the RSAM evolution) at the end of distal eruptions when the deeper magma are involved (Fig. 7). The absence of significant vertical magma migration for the distal eruptions may be related to the high olivine content ($>20\%$ of megacrysts, oceanitic lavas) in the magma, which increases magma density, favouring a deeper lateral migration towards the flank from the base of the shallow reservoir (Fig. 8). Rapid magma ascent at the end of a cycle could be caused by a rapid pulse of magma in the shallow reservoir or/and by the destabilization of the unbuttressed eastern flank.

Each eruptive cycle ends with a distal, large volume of magma ($13\text{ to }100 \times 10^6\text{ m}^3$), oceanite eruption, which drains the shallow plumbing system. Summit deflation results to mechanical and thermal readjustments of the zone surrounding the magma feeding pathways.

6.2. Evolution of the feeding plumbing system

6.2.1. Eruption feeding pathways

For the two eruptive periods (1972–1992 and 1998–2007), magmas systematically migrated towards the surface through the summit zone. Each eruption is preceded by vertical magma ascent below the Dolomieu crater (Peltier et al., 2005). The eruptive cycle pattern described above for 2000–2007 is in agreement with the presence of two preferential vertical dyke pathways below the Dolomieu crater. In a state of structural stability, dykes are initiated below the western part of the Dolomieu due to a favoured rupture at the top of the magma reservoir (i.e. below the western part of the Dolomieu). In contrast, in an unstable state dykes are initiated below the eastern part of Dolomieu crater, influenced by the unbuttressed eastern flank of Piton de La Fournaise, leading thus to distal eruptions (Figs. 6 and 8; Peltier et al., 2007). Although the lack of deformation measurements before 1980 prevented a detailed analysis of pre-1980 eruptive activity, the opening of an eruptive fissure in the eastern part of the Dolomieu crater in the early stage of the April 1977 distal eruption suggests a vertical magma transport below the eastern side of the Dolomieu crater before the propagation of the dyke towards the north-eastern flank, as observed for more recent distal eruptions. Transport of magma through the eastern side of the Dolomieu in 1977 would be in agreement with a recharging of the shallow magma storage before April 1977, which destabilized the unbuttressed eastern flank of the volcano. Due to the lack of geophysical recordings in 1977, we have not strong evidence of such a refilling at this time.

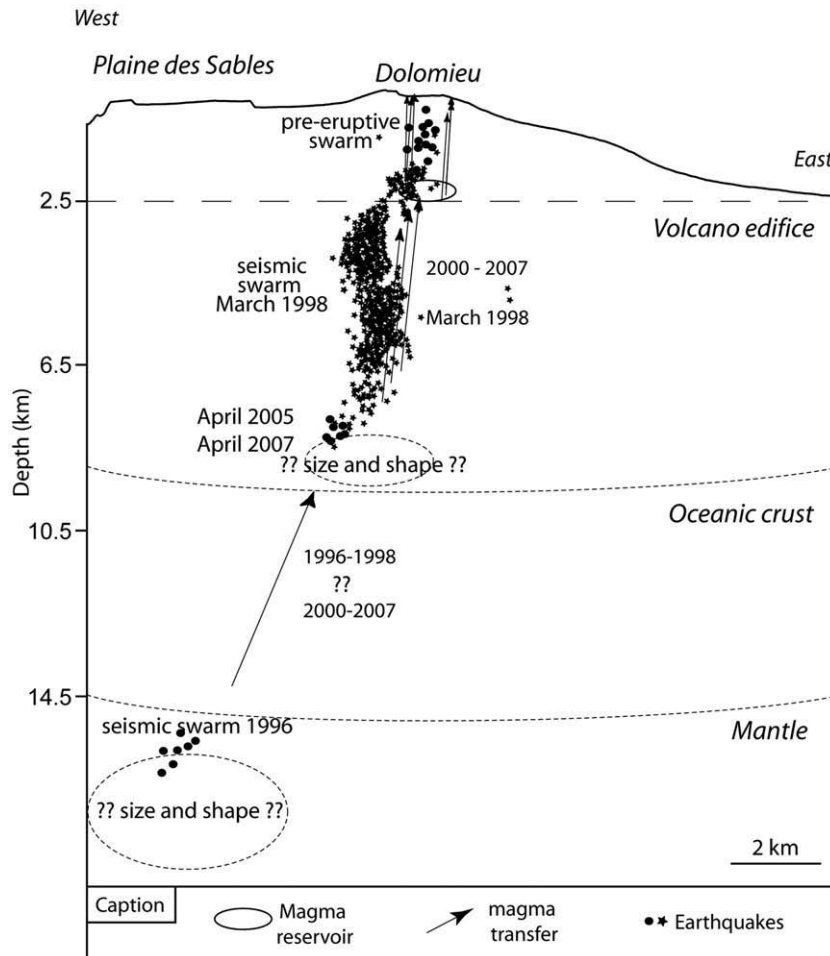


Fig. 9. East-west cross section through Piton de La Fournaise showing the location of earthquakes and magma storage at depth. Location of the March 1998 pre-eruptive seismic swarm (stars) after Battaglia et al. (2005).

By contrast, the 1972–1992 proximal eruptions have been fed by dykes that originated below the western part of the Dolomieu crater (Fig. 1c), which testifies to the stability of the volcano during these periods.

The two preferred vertical feeding pathways below the Dolomieu crater correspond on the surface to the location of the small pit-craters formed in 1953 and 2002 to the west and in 1986 to the east of the crater. Indeed small residual magma pockets may be trapped during the vertical magma ascent below the Dolomieu crater, which, when drained, may lead to the formation of pit craters (Hirn et al., 1991; Longpré et al., 2007). Such events occurred in 1986 and 2002 after major distal eruptions.

6.2.2. Storage system

At least three magma reservoirs have been identified beneath the volcano: 1) at about sea level beneath Dolomieu crater, 2) at the boundary between the volcano and the ocean crust about 7.5 km beneath the volcano, and 3) at about 15 km beneath La Plaine des Sables (~6 km north-west of the summit cone, Fig. 1c).

All post-2000 eruptive and intrusive activity indicates that magma passes through the same shallow magma reservoir located around sea level (2.3 km depth) below the Dolomieu crater (Fig. 8; Peltier et al., 2007, 2008). Sea level could be a major geological discontinuity and may correspond to a neutral buoyancy level where the magma density equals that of the surrounding host rock, favouring magma storage (Battaglia et al., 2005). The presence of a magma reservoir at this level is also suggested by the presence of a low seismic velocity zone just below sea level (Nercessian et al., 1996; Sapin et al., 1996). Moreover, pre-eruptive seismicity (located between 500 to 2500 m depth) is consistently located above sea level. The location of this seismic activity marks the highest stress zone, where the overpressurized magma reservoir generates fractures in the host rock. The core of the reservoir, is probably molten and therefore aseismic. Numerical models suggest a reservoir size of about 0.30 km³ (Peltier et al., 2007), in agreement with the magma production rate (Albarède, 1993) and U-series disequilibria (Sigmarsson et al., 2005) which found volumes of 0.1 to 0.3 km³ and 0.35 km³, respectively.

Studies based on 1977–1988 activity favoured short-term magma storage in a shallow network of interconnected dykes and sills and deeper large magmas bodies (Lénat and Bachèlery, 1990). However the shape of the shallow storage system must be relatively simple to transmit the progressive changes in the volcano's parental magma composition observed during recent eruptions. According to Pietruszka and Garcia (1999), in a geometrically complex magma reservoir (such as a plexus of sills and dykes), the geochemical signature of a particular lava will depend on a number of factors, including the portion of the reservoir tapped by the eruption, the residence time of the magma prior to eruption, and the degree of interaction between magmas in different pockets of the reservoir. Changes in any of these parameters between different eruptions would destroy any systematic temporal variations in parental magma composition. As a result, we favour one main magma reservoir rather than a network of interconnected magma pockets.

After 2000, the shallow reservoir was regularly recharged by magma from a deeper source. The top of the oceanic crust has been recognized as a major geological discontinuity (Gallard et al., 1999) which may favour magma accumulation and storage (Fig. 9), and that location corresponds to both the root of the seismic swarms (about 7.5 km depth) that preceded the 1998 eruption (Battaglia et al., 2005) and the location of a few of the earthquakes recorded in April 2005 and April 2007 (Fig. 9). The connection between this reservoir and the "sea level" reservoir was highlighted in 1998 by deep seismicity beneath the Bory crater. Since the opening of a conduit between the two reservoirs in 1998 (Battaglia et al., 2005), the recharging has occurred aseismically via this warm conduit.

The September 1996 seismic swarm at 15 km depth below La Plaine des Sables could indicate the presence of a third magma reservoir. This reservoir could be an extension of the seismic low velocity anomaly described by Driad (1997) in the south-western part of La Réunion at the

interface of the oceanic crust and the mantle (around 15 km depth), and interpreted as magmatic underplating (Fig. 9).

7. Conclusion

The last 35 years of eruptive activity at Piton de La Fournaise highlights two main eruptive periods lasting several decades and separated by a repose period of six years:

- (1) 1972–1992 characterized by weak seismic and ground deformation eruptive precursors.
- (2) 1998–2007 characterized, after 2000, by a change in the behaviour of the volcano, with continuous summit inflation, strong pre-eruptive seismicity and distal low-altitude eruptions of oceanite lavas alternating with summit and proximal eruptions emitting poorly phyrhic basalts.

The change in the behaviour of Piton de La Fournaise volcano occurred in 2000, two years after the 1998 eruption; which was the first eruption since the implementation of the observatory that was preceded by a deep (~7.5 depth) seismicity emphasizing the arrival of new magma into the shallow reservoir. The opening of a conduit between the shallow reservoir and a deeper one facilitated the transit of the deep magma and modified the general behaviour of the volcano. Within the 2000–2007 period we have defined five eruptive cycles; each cycle is characterized by a sequence of summit and proximal eruptions ending with a distal eruption on the eastern flank, during which emitted lavas are increasingly MgO-rich. We propose that the change in the magma system since 2000 was caused by continuous recharge of the shallow magma reservoir by a deeper one. This continuous recharge would destabilize the volcano's eastern flank favouring distal eruptions towards this flank at the end of each cycle. By contrast, the 1972–1992 period was characterized by the progressive drainage of the shallow magma reservoir, which was occasionally recharged. Geophysical evidence of shallow magma reservoir recharge was only recorded in 1986 and 1998 but would have also occurred in 1972 and 1977.

Acknowledgements

We are grateful to the successive head-scientists, scientists, engineers and technicians who worked at the OVPF since 1980 for their contribution in the follow up of the activity. From 1980 to 2007, the head-scientists at OVPF were successively: F.X. Lalanne, J.F. Lénat, H. Delorme, J.P. Toutain, J. R. Grasso, P. Bachèlery and T. Staudacher. We thank Mike Poland, Brian Upton and Laurent Michon for helpful reviews and comments, which greatly improve the quality of the manuscript. This is IGP contribution number 2467.

References

- Albarède, F., 1993. Residence time analysis of geochemical fluctuations in volcanic series. *Geochim. Cosmochim. Acta* 57, 615–621.
- Albarède, F., Tamagnan, V., 1988. Modelling the recent geochemical evolution of the Piton de La Fournaise volcano, Réunion Island, 1931–1986. *J. Petrol.* 29 (5), 997–1030.
- Albarède, F., Luais, B., Fitton, G., Semet, M., Kaminski, E., Upton, B.G.J., Bachèlery, P., Cheminée, J.L., 1997. The geochemical regimes of Piton de La Fournaise volcano (Réunion) during the last 530,000 years. *J. Petrol.* 38 (2), 171–201.
- Allard, P., Behncke, B., D'Amico, S., Neri, M., Gambino, S., 2006. Mount Etna 1993–2005: anatomy of an evolving eruptive cycle. *Earth-Sci. Rev.* 78, 85–114.
- Augier, A., Froger, J.L., Cayol, V., Fukushima, Y., Tinard, P., Souriot, T., Mora, O., Staudacher, T., Durand, P., Fruneau, B., Villeneuve, N., 2008. The April 2007 eruption at Piton de la Fournaise, Réunion Island, imaged with ENVISAT-ASAR and ALOS-PALSAR data, USRESt workshop, Napoli, Italy.
- Bachèlery, P., 1981. Le Piton de La Fournaise (île de La Réunion). Etude volcanologique structurale. PhD Thesis, Université de Clermont Ferrand.
- Bachèlery, P., 1999. Le Fonctionnement des volcans boucliers. HDR Thesis, Université de La Réunion.
- Bachèlery, P., Mairine, P., 1990. Evolution volcano-structurale du Piton de La Fournaise depuis 0.53 Ma. In: Lénat, J.-F. (Ed.), Le volcanisme de La Réunion. Centre de Recherches Volcanologiques, Clermont-Ferrand, pp. 213–242.

- Bachèlery, P., Blum, P.A., Cheminée, J.L., Chevallier, L., Gaulon, R., Girardin, N., Jaupart, C., Lalanne, F., Le Mouel, J.L., Ruegg, J.C., Vincent, P., 1982. Eruption at Le Piton de La Fournaise volcano on 3 February 1981. *Nature* 297 (5865), 395–397.
- Battaglia, J., Bachèlery, P., 2003. Dynamic dyke propagation deduced from tilt variations preceding the March 9, 1998, eruption of the Piton de La Fournaise volcano. *J. Volcanol. Geotherm. Res.* 120, 289–310.
- Battaglia, J., Ferrazzini, V., Staudacher, T., Aki, K., Cheminée, J.L., 2005. Pre-eruptive migration of earthquakes at the Piton de La Fournaise volcano (Réunion Island). *Geophys. J. Int.* 161, 549–558.
- Blake, S., 1981. Volcanism and the dynamics of open magma chambers. *Nature* 289, 783–785.
- Boivin, P., Bachèlery, P., 2004. The behaviour of the shallow plumbing system at La Fournaise volcano (Réunion Island): a petrological approach, EGS-AGU-EUG Joint Assembly, Nice, France.
- Boivin, P., Bachèlery, P., 2009. Petrology of 1977 to 1998 eruptions of Piton de La Fournaise, La Réunion Island. *J. Volcanol. Geotherm. Res.* 184, 109–125 (this issue).
- Bosch, D., Blichert-Toft, J., Moynier, F., Nelson, B.K., Telouk, P., Gillot, P.-Y., Albarède, F., 2008. Pb, Hf and Nd isotope compositions of the two Réunion volcanoes (Indian Ocean): a tale of two small-scale mantle “blobs”? *Earth Planet. Sci. Lett.* 65, 748–768.
- Brenguier, F., Shapiro, N.M., Campillo, M., Ferrazzini, V., Duputel, Z., Coutant, O., Nercessian, A., 2008. Towards forecasting volcanic eruptions using seismic noise. *Nat. Geosci.* 1, 126–130.
- Briole, P., Bachèlery, P., Mc Guire, B., Moss, J., Ruegg, J.C., Sabourault, Ph., 1998. Deformation of Piton de La Fournaise: evolution of the monitoring techniques and knowledge acquired in the last five years. In: Casale, R., et al. (Ed.), *The European Laboratory Volcanoes, Second Workshop Santorini, Greece*.
- Bureau, H., Métrich, N., Semet, M., Staudacher, T., 1999. Fluid magma decoupling in a hot-spot volcano. *Geophys. Res. Lett.* 26 (23), 3501–3504.
- Carter, A., Van Wyk de Vries, B., Kelfoun, K., Bachèlery, P., Briole, P., 2007. Pits, rifts and slumps: the summit structure of Piton de La Fournaise. *Bull. Volcanol.* 69, 741–756.
- Cayol, V., Cornet, F.H., 1997. 3D mixed boundary elements for elastostatic deformation field analysis. *Int. J. Rock Mech. Min. Sci.* 34 (2), 275–287.
- Cayol, V., Cornet, F.H., 1998. Three-dimensional modelling of the 1983–1984 eruption at Piton de La Fournaise Volcano, Reunion Island. *J. Geophys. Res.* 103 (B8), 18025–18037.
- Clague, D.A., Denlinger, R.P., 1994. Role of olivine cumulates in destabilizing the flanks of Hawaiian volcanoes. *Bull. Volcanol.* 54, 425–434.
- Coombs, D.S., 1963. Trends and affinities of basaltic magmas and pyroxenes as illustrated on the diopside-olivine-silica diagram. *Spec. Pap. - Miner. Soc. Am.* 1, 227–250.
- Delorme, H., 1994. Apport des déformations à la compréhension des mécanismes éruptifs: le Piton de La Fournaise. Doctorat d'état thesis. Université Paris VII.
- Delorme, H., Bachèlery, P., Blum, P.A., Cheminée, J.-L., Delarue, J.-F., Delmond, J.-C., Hirn, A., Lépine, J.-C., Vincent, P.-M., Zlotnicki, J., 1989. March 1986 eruptive episodes at Piton de La Fournaise volcano (Réunion Island). *J. Volcanol. Geotherm. Res.* 36, 199–208.
- Driad, L., 1997. Structure profonde de l'édifice volcanique de La Réunion (océan Indien) par sismique réfraction et grand angle. PhD Thesis, Université de Paris VII.
- Duffield, W.E., Stieltjes, L., Varet, J., 1982. Huge landslide blocks in the growth of Piton de La Fournaise, La Réunion, and Kilauea volcano, Hawaii. *J. Volcanol. Geotherm. Res.* 12, 147–160.
- Famin, V., Welsch, B., Okumura, S., Bachèlery, P., Nakashima, S., 2008. Three differentiation stages of a single magma at Piton de la Fournaise (Reunion hotspot). *G-Cubed*. doi:10.1029/2008GC002015.
- Fisk, M.R., Upton, B.G.J., Ford, C.E., White, W.M., 1988. Geochemical and experimental study of the genesis of magmas of Réunion Island, Indian Ocean. *J. Geophys. Res.* 93, 4933–4950.
- Froger, J.-L., Fukushima, Y., Briole, P., Staudacher, T., Souriot, T., Villeneuve, N., 2004. The deformation field of the August 2003 eruption at Piton de La Fournaise, Reunion Island, mapped by ASAR interferometry. *Geophys. Res. Lett.* 31 (14). doi:10.1029/2004GL020479.
- Fukushima, Y., 2005. Transferts de magma au volcan du Piton de La Fournaise déterminés par la modélisation 3D de données d'interférométrie radar entre 1998 et 2000. PhD Thesis, Université de Clermont Ferrand.
- Fukushima, Y., Cayol, V., Durand, P., 2005. Finding realistic dike models from interferometric synthetic aperture radar data: the February 2000 eruption at Piton de La Fournaise. *J. Geophys. Res.* 110 (B03206). doi:10.1029/2004JB003268.
- Gallard, J., Driad, L., Charvis, P., Sapin, M., Hirn, A., Diaz, J., de Voogd, B., Sachpazi, M., 1999. Perturbation to the lithosphere along the hotspot track of La Réunion from an offshore-onshore seismic transect. *J. Geophys. Res.* 104 (B2), 2895–2908.
- Graham, D., Lupton, J., Albarède, F., Comdomines, M., 1990. Extreme temporal homogeneity of helium isotopes at Piton de la Fournaise, Reunion Island. *Nature* 347, 545–548.
- Hirn, A., Lépine, J.-C., Sapin, M., Delorme, H., 1991. Episodes of pit-crater collapse documented by seismology at Piton de la Fournaise. *J. Volcanol. Geotherm. Res.* 47, 89–104.
- Kieffer, G., Tricot, B., Vincent, P.M., 1977. Une éruption inhabituelle (avril 1977) du Piton de La Fournaise (Ile de La Réunion): ses enseignements volcanologiques et structuraux. *C. R. Acad. Sci. Paris* 285 D, 957–960.
- Krafft, M., Gerente, A., 1977. L'activité du Piton de la Fournaise entre octobre 1972 et mai 1973. (Ile de La Réunion, Océan Indien). *C. R. Acad. Sci. Paris* 284 D, 607–610.
- Lacroix, A., 1912. Les laves du volcan actif de la Réunion. *C. R. Acad. Sci. Paris* T154, 251–257.
- Lénat, J.F., Bachèlery, P., 1987. Dynamics of magma transfer at Piton de La Fournaise Volcano (Réunion Island, Indian Ocean). In: Chi-Yu, Scarpa (Eds.), *Earth Evolution Sciences* (Special Issue “Modeling of Volcanic Processes”. Friedr. Vieweg and Sohn, Braunschweig, pp. 57–72.
- Lénat, J.-F., Bachèlery, P., 1990. Structure et fonctionnement de la zone centrale du Piton de La Fournaise. In: Lénat, J.-F. (Ed.), *Le volcanisme de La Réunion*. Centre de Recherches Volcanologiques, Clermont-Ferrand, pp. 257–296.
- Lénat, J.-F., Bachèlery, P., Bonneville, A., Hirn, A., 1989a. The beginning of the 1985–1987 eruptive cycle at Piton de La Fournaise (La Réunion); new insights in the magmatic and volcano-tectonic systems. *J. Volcanol. Geotherm. Res.* 36, 209–232.
- Lénat, J.-F., Bachèlery, P., Bonneville, A., Tarits, P., Cheminée, J.-L., Delorme, H., 1989b. The December 4, 1983 to February 18, 1984 eruption of Piton de La Fournaise (La Réunion, Indian ocean): description and interpretation. *J. Volcanol. Geotherm. Res.* 36, 87–112.
- Lénat, J.-F., Vincent, P., Bachèlery, P., 1989c. The off-shore continuation of an active basaltic volcano: Piton de La Fournaise (Reunion Island, Indian Ocean); structural and geomorphological interpretation from sea beam mapping. *J. Volcanol. Geotherm. Res.* 36, 1–36.
- Lénat, J.-F., Gilbert-Malengreau, B., Galdéano, A., 2001. A new model for the evolution of the volcanic island of Réunion (Indian Ocean). *J. Geophys. Res.* 106 (B5), 8645–8663.
- Longpré, M.A., Staudacher, T., Stix, S., 2007. The November 2002 eruption at Piton de La Fournaise volcano, La Reunion Island: ground deformation, seismicity, and pit crater collapse. *Bull. Volcanol.* 69, 511–525.
- Ludden, J.N., 1978. Magmatic evolution of the basaltic shield volcanoes of Reunion Island. *J. Volcanol. Geotherm. Res.* 4 (1/2), 171–198.
- Mériaux, C., 1996. Transport de magma dans les filons Thèse de doctorat Thesis, Institut de Physique du Globe de Paris - Université de Paris 7.
- Michon, L., Saint-Ange, F., Bachèlery, P., Villeneuve, N., Staudacher, T., 2007a. Role of the structural inheritance of the oceanic lithosphere in the magmato-tectonic evolution of Piton de La Fournaise volcano (La Réunion Island). *J. Geophys. Res.* 112 (B04205). doi:10.1029/2006JB004598.
- Michon, L., Staudacher, T., Ferrazzini, V., Bachèlery, P., Marti, J., 2007b. April 2007 collapse of Piton de La Fournaise: a new example of caldera formation. *Geophys. Res. Lett.* 34 (L21301) 1029/2007GL031248.
- Nercessian, A., Hirn, A., Lépine, J.-C., Sapin, M., 1996. Internal structure of Piton de La Fournaise volcano from seismic wave propagation and earthquakes distribution. *J. Volcanol. Geotherm. Res.* 70, 123–143.
- Okada, Y., 1985. Surface deformation due to shear and tensile faults in a half space. *Bull. Seismol. Soc. Am.* 75, 1135–1154.
- Peltier, A., 2007. Suivi, Modélisation et Evolution des processus d'injections magmatiques au Piton de La Fournaise. PhD Thesis, Université de La Réunion. 365 pp.
- Peltier, A., Ferrazzini, V., Staudacher, T., Bachèlery, P., 2005. Imaging the dynamics of dyke propagation prior to the 2000–2003 flank eruptions at Piton de La Fournaise, Reunion Island. *Geophys. Res. Lett.* 32 (L22302). doi:10.1029/2005GL023720.
- Peltier, A., Staudacher, T., Catherine, P., Ricard, L.-P., Kowalski, P., Bachèlery, P., 2006. Subtle precursors of volcanic eruptions at Piton de la Fournaise detected by extensometers. *Geophys. Res. Lett.* 33 (L06315). doi:10.1029/2005GL025495.
- Peltier, A., Staudacher, T., Bachèlery, P., 2007. Constraints on magma transfers and structures involved in the 2003 activity at Piton de La Fournaise from displacement data. *J. Geophys. Res.* 112 (B03207). doi:10.1029/2006JB004379.
- Peltier, A., Famin, V., Bachèlery, P., Cayol, V., Fukushima, Y., Staudacher, T., 2008. Cyclic magma storages and transfers at Piton de La Fournaise volcano (La Réunion hotspot) inferred from deformation and geochemical data. *Earth Planet. Sci. Lett.* 270 (3–4), 180–188.
- Pietruszka, A.J., Garcia, M.O., 1999. The size and shape of Kilauea volcano's summit magma storage reservoir: a geochemical probe. *Earth Planet. Sci. Lett.* 167, 311–320.
- Pinel, V., Jaupart, C., 2004. Magma storage and horizontal dyke injection beneath a volcanic edifice. *Earth Planet. Sci. Lett.* 221, 245–262.
- Sapin, M., Hirn, A., Lépine, J.-C., Nercessian, A., 1996. Stress, failure and fluid flow deduced from earthquakes accompanying eruptions at Piton de La Fournaise volcano. *J. Volcanol. Geotherm. Res.* 70, 145–167.
- Sigmarsson, O., Condomines, M., Bachèlery, P., 2005. Magma residence time beneath the Piton de La Fournaise Volcano, Reunion Island, from U-series disequilibria. *Earth Planet. Sci. Lett.* 234, 223–234.
- Sigmundsson, F., Durand, P., Massonet, D., 1999. Opening of an eruption fissure and seaward displacement at Piton de La Fournaise volcano measured by RADARSAT satellite radar interferometry. *Geophys. Res. Lett.* 26, 533–536.
- Staudacher, T., Sarda, P., Allègre, C.J., 1990. Noble gas systematics of Réunion Island, Indian Ocean. *Chemical Geology* 89, 1–17.
- Staudacher, T., Ferrazzini, V., Peltier, A., Kowalski, P., Boissier, P., Catherine, P., Lauret, F., Massin, F., 2009. The April 2007 eruption and the Dolomieu crater collapse, two major events at Piton de la Fournaise (La Réunion Island, Indian Ocean). *J. Volcanol. Geotherm. Res.* 184, 126–137 (this issue). doi:10.1016/j.jvolgeores.2008.11.005.
- Tait, S., Jaupart, C., Vergnolle, S., 1989. Pressure, gas content and eruption periodicity of a shallow, crystallizing magma chamber. *Earth Planet. Sci. Lett.* 92, 107–123.
- Toutain, J.-P., Bachèlery, P., Blum, P.-A., Cheminée, J.L., Delorme, H., Fontaine, L., Kowalski, P., Tauchy, P., 1992. Real time monitoring of vertical ground deformations during eruptions at Piton de la Fournaise. *Geophys. Res. Lett.* 19 (6), 553–556.
- Tinard, P., 2007. Caractérisation et modélisation des déplacements du sol associés à l'activité volcanique du Piton de La Fournaise, île de La Réunion, à partir de données interférométriques. Août 2003 – Avril 2007. PhD Thesis, Université de Clermont Ferrand. 334 pp.
- Upton, B.G.J., Wadsworth, W.J., 1965. Geology of Réunion Island, Indian Ocean. *Nature* 207, 151–154.
- Upton, B.G.J., Wadsworth, W.J., 1966. The basalts of Réunion Island, Indian Ocean. *Bull. Volcanol.* 29, 7–23.
- Upton, B.G.J., Wadsworth, W.J., 1972. Aspects of magmatic evolution on Reunion Island. *Philos. Trans. R. Soc. Lond.*, A 271, 105–130.

- Upton, B.G.J., Semet, M.P., Joron, J.-L., 2000. Cumulate clasts in the Bellecombe Ash Member, Piton de la Fournaise, Réunion Island, and their bearing on cumulative processes in the petrogenesis of the Réunion lavas. *J. Volcanol. Geotherm. Res.* 104, 297–318.
- Vlastélic, I., Staudacher, T., Semet, M., 2005. Rapid change of lava composition from 1998 to 2002 at Piton de La Fournaise (Réunion) inferred from Pb isotopes and trace elements: evidence for variable crustal contamination. *J. Petrol.* 46 (1), 79–107.
- Vlastélic, I., Peltier, A., Staudacher, T., 2007. Short-term (1998–2006) fluctuations of Pb isotopes at Piton de la Fournaise volcano (Reunion Island): origins and constrains on the size and shape of the magma reservoir. *Chem. Geol.* 244, 202–220.
- Vlastélic, I., Deniel, C., Bosq, C., Télouk, P., Boivin, P., Bachèlery, P., Famin, V., Staudacher, T., 2009. Pb isotope geochemistry of Piton de La Fournaise historical lavas. *J. Volcanol. Geotherm. Res.* 184, 63–78 (this issue). doi:10.1016/j.jvolgeores.2008.08.008.
- Zlotnicki, J., Ruegg, J.C., Bachèlery, P., Blum, P.A., 1990. Eruptive mechanisms on Piton de la Fournaise volcano associated with the December 4, 1983, and January 18, 1984, eruptions from ground deformation monitoring and photogrammetric surveys. *J. Volcanol. Geotherm. Res.* 40, 197–217.